Accelerating Cleanup of the Defense Nuclear Legacy

Quarterly Technical Progress Report for the period
January – March 2009

Dr. Jeff Lindner, Principal Investigator

Report No. 07040R09

Prepared for the U.S. Department of Energy
Agreement No. DE-FC01-06EW-07040

Institute for Clean Energy Technology
Mississippi State University
205 Research Boulevard
Starkville, MS 39759

lindner@icet.msstate.edu
www.icet.msstate.edu

Acknowledgement
This material is based upon work supported by the Department of Energy under award number DE-FC01-06EW-07040

Table of Contents

List of Figures

List of Tables

EXECUTIVE SUMMARY

Task 1: Efforts Directed toward Savannah River

Task 1.1: Thermodynamic data and computational methods for liquid waste flowsheet modeling

ESP simulations were conducted which evaluated the recovery of SRS Tank 38H saltcake using DWPF recycle for dissolution and Batch 5 leachate for corrosion control. Stream compositions and properties were predicted for 0 to 100 % (wt.) dissolution. As expected from the high level of nitrate in the initial saltcake solids, the Na^+, OH^-, NO_3^-, and NO_2^- ions dominate most of the dissolution. As 100 % (wt.) dissolution is approached, $Na_2C_2O_4$ replaces $NaNO_3$ as the major remaining solid and at 100 % (wt.) dissolution, no $NaNO_3$ remains in the saltcake. An evaluation of dissolution transfer streams as per adherence to corrosion specifications show that corrosion compliance is maintained for dissolutions below 40 % (wt.) dissolution. The addition of Batch 5 leachate to streams above 40 % dissolution was effective in reaching corrosion minimum specifications. However, streams from higher dissolutions require up to 20% (volume) leachate addition to achieve corrosion specifications. In addition, dissolution streams, after corrosion compliance was achieved, were cooled to simulate storage conditions. These simulations predict higher levels of solids precipitation in streams without leachate addition. Finally, cool, corrosion compliant, dissolution streams were introduced to the CSSX scrub section to predict solids precipitation from waste stream carryover. At 10% dissolution, 0.02 % (wt.) solids, $Al(OH)_3$, is predicted for pH values above 3. For higher dissolution streams approximately 0.04 % (wt.) solids are predicted above a pH of 3. However, $NaAlCO_3(OH)_2$ is indicated as the only solid between pH values of 6 and 10.5. At all other pH values, above 3, $Al(OH)_3$ is the only predicted solid. At pH values below 3, essentially zero solids precipitation, 10^{-7} % (wt.) solids, was indicated.

Task 1.2: SRS Saltstone Process Studies

The construction of an adiabatic calorimeter is complete and the process of testing the instrument is now underway. Important aspects of this testing includes temperature control of the water bath, voltage control of the heater, tracking of the sample temperature by the bath temperature, data acquisition, and overall instrument operation. Using raw materials (Portland cement, fly ash, and blast furnace slag) left over from previous projects, the testing has taken recipes from previous Savannah River reports to check out instrument operation.

Task 2: Support of Hanford Alternatives and Tank Closure

Task 2.1: Aluminum Solubility

Information on important constituents found within WTP solutions in feed to ion exchange was obtained from site personnel and after discussion of the reported concentration ranges,

temperatures, and caustic levels, a test plan was developed. The test plan was written and reviewed to establish experimental design for aluminum solubility with selected sodium components and caustic loadings at temperatures of interest during the stages of WTP sludge caustic leaching and processing of the resulting streams.

Task 2.2: In-Tank Characterization for Closure of Hanford Waste Tanks

A fresh characterization of the inherent and instrumental uncertainties associated with the current FTP system has begun. This was necessary because previous characterization of FTP instrumental response had been performed over the years with a variety of different equipment and different experimental configurations, rendering comparisons and generalized quantitative conclusions difficult.

Task 3: EM-21 Cross-cutting Activities

Task 3.1 Laser Induced Breakdown Spectroscopy: Application to Nuclear Waste Management

Laser induced breakdown spectroscopy (LIBS) is a diagnostic technique that can measure the concentrations of various elements in a test sample. This project evaluates the applications of LIBS to waste characterization and processing within the DOE complex. During this work period, we have evaluated the effects of water content to the LIBS slurry measurement. Various sample preparation techniques were evaluated to improve LIBS measurement quality by reducing water content in slurry.

Task 3.2 Evaluation of HEPA Filters Under Fire (High Soot Loading) Conditions

HEPA filters are used as the final element in nearly all containment systems where radioactive wastes are processed. Data are needed to aid in the development of loading models to incorporate the effects of both water damage and filter blinding on full size (24x24x11.5”) as well as radial (ASME Standard AG-1, Section FK) filters. A new HEPA filter test facility has been designed at ICET to accommodate a nominal flow rate of 4000 scfm and allow for a differential pressure drop across a HEPA filter of 30 in.wc.

Task 1

Efforts Directed toward Savannah River

Thermodynamic data and computational methods for liquid waste flowsheet modeling

Larry Pearson, Laura Smith, John Luthe, and Jeff Lindner

INTRODUCTION

Development of the Salt Waste Processing Facility (SWPF) at the Savannah River Site (SRS) is expected to permit separation of actinides and cesium from the non-radioactive components of the waste. The high activity waste will be routed to the Defense Waste Processing Facility (DWPF) for immobilization in glass, while the low activity waste will be stabilized as saltstone. Two main processes are contained within the SWPF, the actinide removal process, (ARP) and Caustic Side Solvent Extraction (CSSX).

In preparation for the planned start up of the full-scale SWPF in 2011, a number of efforts are addressing waste acceptance criteria and the performance of individual unit operations [1, 2]. Most of the SRS waste streams, with the exception of high activity sludge batches destined for the DWPF, will be processed through the SWPF. Some of these streams include various stage fractions from saltcake dissolution, supersaturated aluminum streams generated from sludge leaching, and the DWPF Recycle stream that emanates from overheads associated with vitrification. Associated compositions of these streams, either alone or blended together, will have a direct impact on the stability of the waste within the SWPF. This impact can be assessed through thermodynamic modeling as well as experimental studies specifically designed to examine solids re-precipitation.

Previous ICET efforts centered on the evaluation of blending strategies for disposition of the streams noted above and characterization of solid samples formed during pilot-scale testing of the CSSX process. This work indicated that the DWPF Recycle stream can be employed as a diluent for saltcake dissolution for waste from SRS Tank 41H [3] and SRS Tank 25F [4]. The ability to blend the high aluminum leachate solution from the sludge leaching process with salt solutions from Tank 25F was also evaluated. Initial results suggest that the Batch 5 leachate can be used for minimizing solids re-precipitation and to aid in corrosion control. The later point would effectively reduce the use of caustic within the tank farm.

This project is divided into 2 tasks. Task 1.1.1 will consist of additional blending simulations on other salt compositions present within the SRS Tank farm. Dissolution of the saltcake using the DWPF Recycle stream will be followed by blending of the dissolved salt fractions with the Batch 5 leachate. Simulation results will be evaluated based on corrosion requirements and existing SWPF waste acceptance criteria. The data will also be evaluated for potential mixing rules, which could improve processing efforts. Simulants will be generated based on blending simulations and evaluated in the laboratory for solids formation. Solids will be identified using polarizing light microscopy, XRD, and ICP.

Task 1.1.2 will provide additional experimental support for CSSX pilot-scale experimentation at Parsons and at ICET. Solids identifications will be performed along with thermodynamic modeling of simulants that will be employed here.

WORK ACCOMPLISHED

This report focuses on the processing of SRS tank 38H from dissolution, through corrosion compliance, and finally through specific parts of the Caustic Side Solvent Extraction (CSSX) process. Predictions of stream compositions and properties were calculated using the OLI Environmental Simulation Program (version 8.0.58 using the V7DBSLT and Corrosion databases). A simple block flow diagram of the entire process, as modeled, is shown in Figure 1. It should be noted that the removal of actinides and strontium by sorption onto monosodium titanate (MST), as planned prior to the CSSX process, was not modeled. In addition, any processing post-CSSX was not considered.

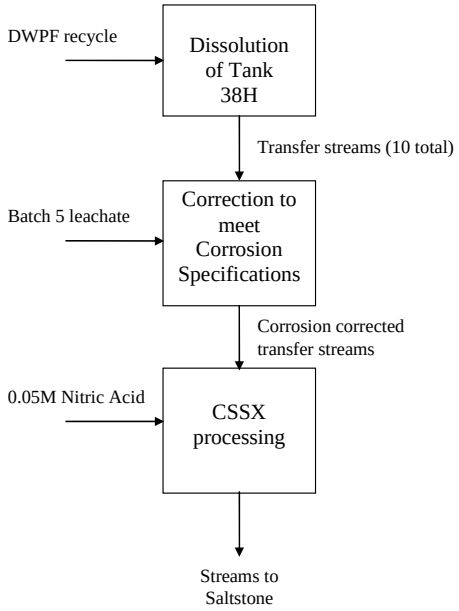

Figure 1 – Simplified Diagram of Processes Modeled

Tank 38H Dissolution

SRS Tank 38H contains a total volume of 309" of saltcake waste and free liquid [5]. Of the total height, 243" is comprised of the undrained saltcake, while the volume above 243" is free liquid. Using data from a previous report, the estimated amount of undrained saltcake and free liquid is 853,000 gallons and 231,707 gallons, respectively [6]. Sampling of the 38H contents have indicated a solids composition as shown in Table 1 and a free liquid composition as shown in Table 2 [5].

Table 1 – SRS Tank 38H Saltcake Solids

Compound	Weight %
$NaNO_3$	84.3
$Na_2CO_3 \cdot H_2O$	10.1
Na_2SO_4	3.7
$Na_2C_2O_4$	1.1
$NaAlO_2 \cdot 2H_2O$	0.8
NaF	0.1

Table 2 – SRS Tank 38H Free Liquid Components

Anion	mg/liter		Cation	mg/liter
NO_3^-	1.29E+05		Al^{+3}	4.30E+03
NO_2^-	8.13E+04		Cr^{+3}	1.33E+02
SO_4^{-2}	2.27E+03		Na^+	2.47E+05
PO_4^{-3}	1.13E+03		Si^{+4}	1.46E+02
Cl^-	1.75E+02			
F^-	0.0			
$C_2O_4^{-2}$	0.0			
CHO_2^-	2.14E+03			
OH^-	9.43E+04			
CO_3^{-2}	1.72E+04			

In addition to the data listed above, it was reported that the undrained saltcake consisted of 16.8% (wt) water with a density of 1.94 g/ml. By comparison, both the free liquid and interstitial liquid consisted of 54.4% (wt) water and had a density of 1.45 g/ml. For purposes of this modeling, the following assumptions were also made:

- undrained saltcake consists of:
  - 60% (vol) solids
  - 30% (vol) liquid
  - 10% (vol) gas (for these simulations, assumed void)

A compilation and charge balancing of the reported data with the above assumptions resulted in a molecular species representation of the Tank 38H composition as shown in Table 3. Table 3 also shows the inclusion of Cs^{137} and Sr^{90} based on the reported activity of the bulk saltcake and free liquid [5].

Table 3 - Tank 38H molecular composition (mole fractions)

Component	Free liquid	Interstitial liquid	Saltcake solids	Total Tank
$Al(OH)_3$	0.002928	0.002928		0.001848
$Cr(OH)_3$	0.000046	0.000046		0.000029
SiO_2	0.000045	0.000045		0.000029
NaOH	0.104360	0.104360		0.065852
$NaNO_3$	0.042555	0.042555	0.821464	0.329968
$NaNO_2$	0.036148	0.036148		0.022809
Na_2SO_4	0.000482	0.000482	0021582	0.008268
Na_3PO_4	0.000244	0.000244		0.000154
NaCOOH	0.000973	0.000973		0.000614
NaCl	0.000103	0.000103		0.000065
Na_2CO_3	0.005865	0.005865	0.067465	0.028595
$Na_2C_2O_4$			0.006799	0.002509
$NaAlO_2$			0.004418	0.001630
NaF			0.001972	0.000728
CsOH				2.11E-07
$Sr(NO_3)_2$				1.64E-08
Water	0.806249	0.806249	0.076300	0.536902

Once the compositions of the 38H saltcake, interstitial liquid, and free liquid had been determined, the dissolution process was modeled as shown in Figure 2. The initial step involved the removal of excess liquid in order to approximate a tank containing only undrained saltcake. Since the modeling assumption was made that the volume of the undrained saltcake was comprised of solids (60%), liquids (30%), and gases (or void, 10%), the result of this step was a 38H composition containing a solids/liquids ratio of 2/1. Following the initial preparation step, the first dissolution stage combined the 38H composition with Defense Waste Processing Facility (DWPF) recycle and allowed the ESP program to calculate chemical equilibrium [4]. The DWPF recycle is a candidate for dissolution of the saltcake as it is a high pH stream that must also be processed. The amount of DWPF recycle added was based on the initial 38H content of undrained saltcake as seen at the end of the preparation step. For this simulation, all additions of DWPF recycle equate to 10% (wt) of the starting amount of undrained saltcake. As in the preparation step, a transfer stream was removed from the resulting liquids to maintain a 2/1 solids-to-liquids ratio for the subsequent dissolution stage. This transfer stream represents the stream that would enter the CSSX process after corrosion control corrections. In this manner, evaluation of the dissolution process was observed from 0% to 100% dissolution, in

increments of 10%. The entire dissolution process was modeled at 30º C and 1 atmosphere pressure.

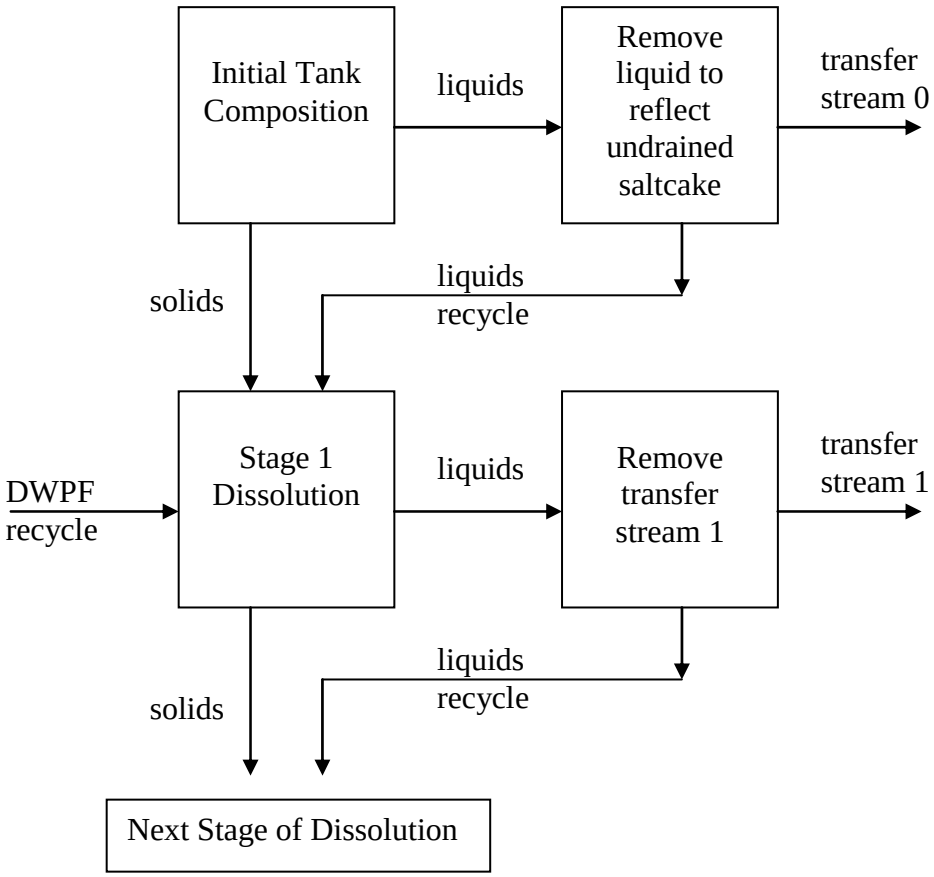

Figure 2 - Flow Diagram of Modeled Dissolution Process

The volume of waste remaining in Tank 38H throughout the dissolution process is shown in Figure 3. The volume shown to the left of 0% dissolution is the initial tank volume with excess free liquid. The volume at 0% dissolution corresponds to initiation of dissolution when the tank contains only the undrained saltcake (i.e. solids plus interstitial liquid).

Figure 4 shows the saltcake solids remaining in 38H during the dissolution. It can be seen that until 80% (wt) dissolution, $NaNO_3$ is the major solids. As the dissolution continues to 100% (wt), $Na_2C_2O_4$ becomes the major solids remaining. Figures 5, 6, 7 and 8 show the composition of the transfer stream as the dissolution process proceeds. As expected from the high level of nitrate in the saltcake solids, the Na, OH, NO_3^-, and NO_2^- ions dominate most of the dissolution. Only at 100% (wt) dissolution is there a shift in this trend. As is seen in Figure 9, a significant change is also observed in the ionic strength.

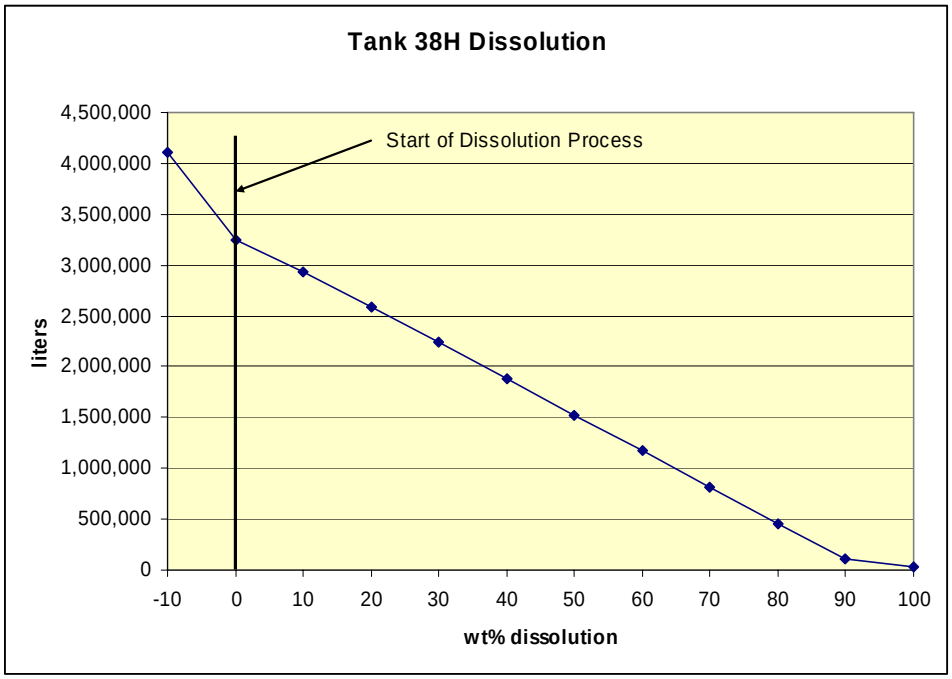

Figure 3 - Tank 38H Volume During Dissolution

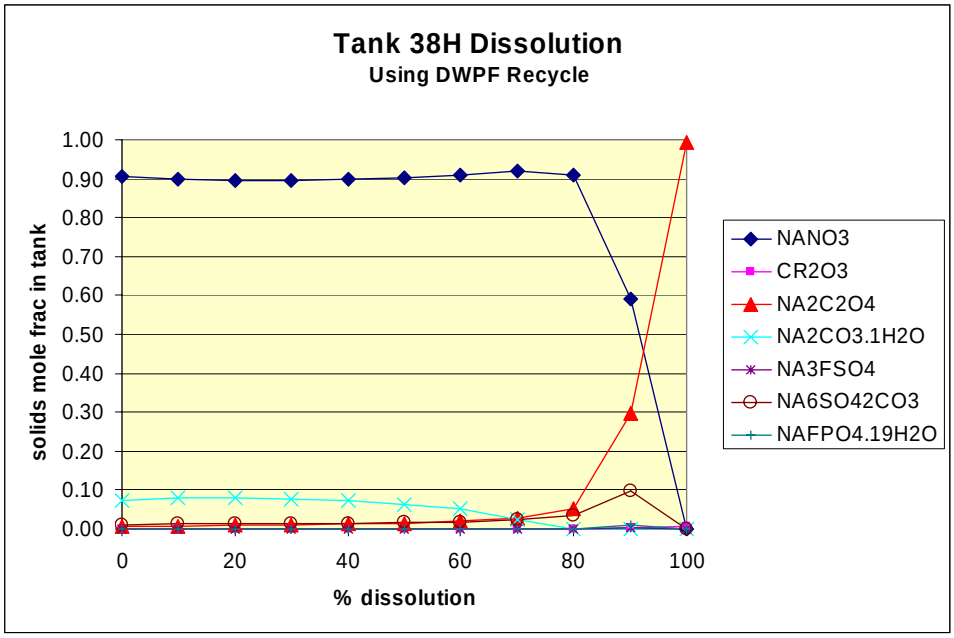

Figure 4 - Tank 38H Saltcake Solids

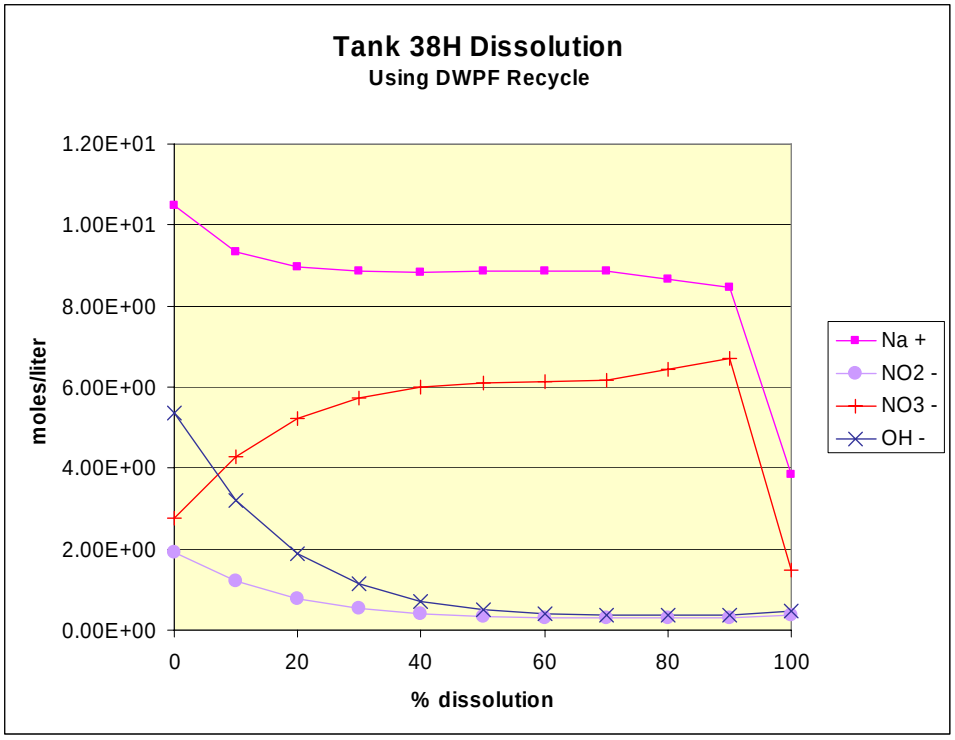

Figure 5 - Tank 38H Transfer Stream Composition

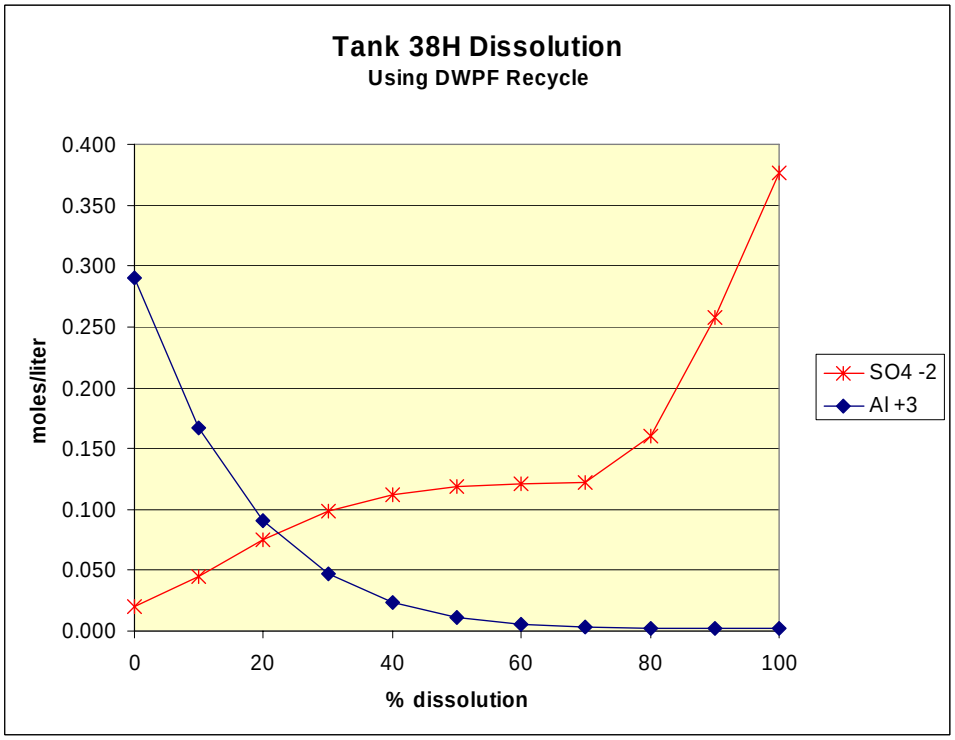

Figure 6 - Tank 38H Transfer Stream Composition

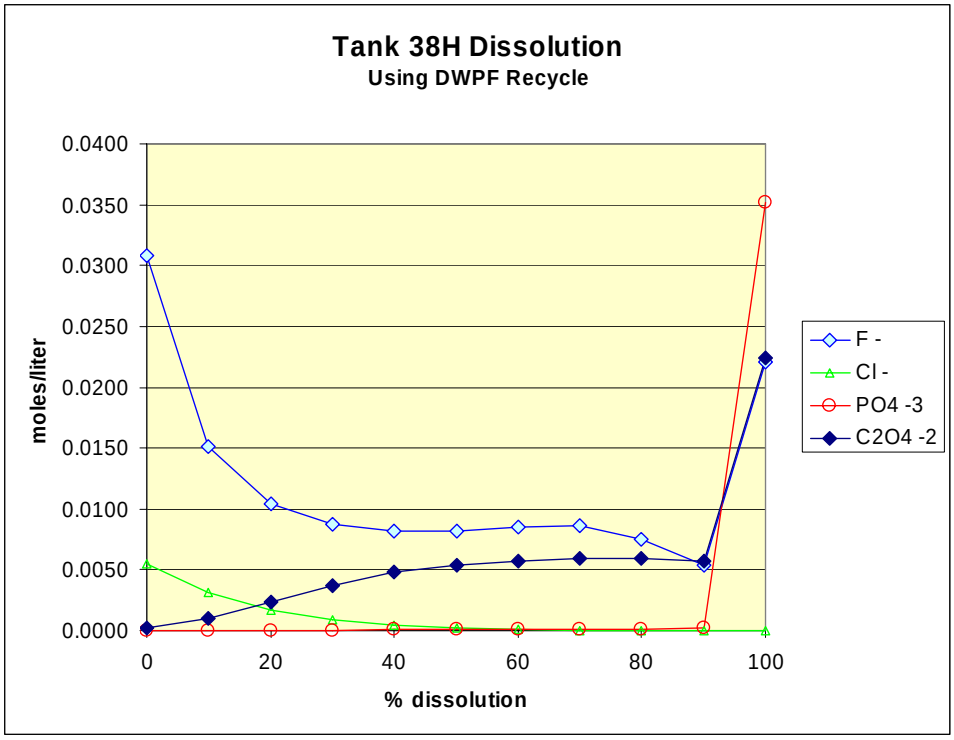

Figure 7 - Tank 38H Transfer Stream Composition

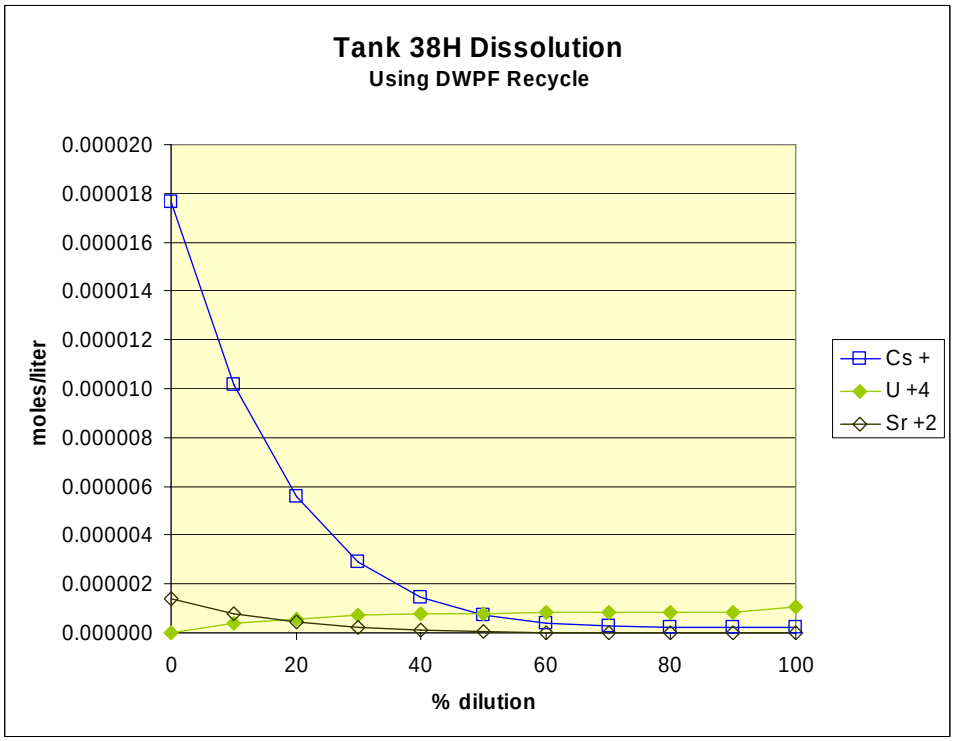

Figure 8 - Tank 38H Transfer Stream Composition

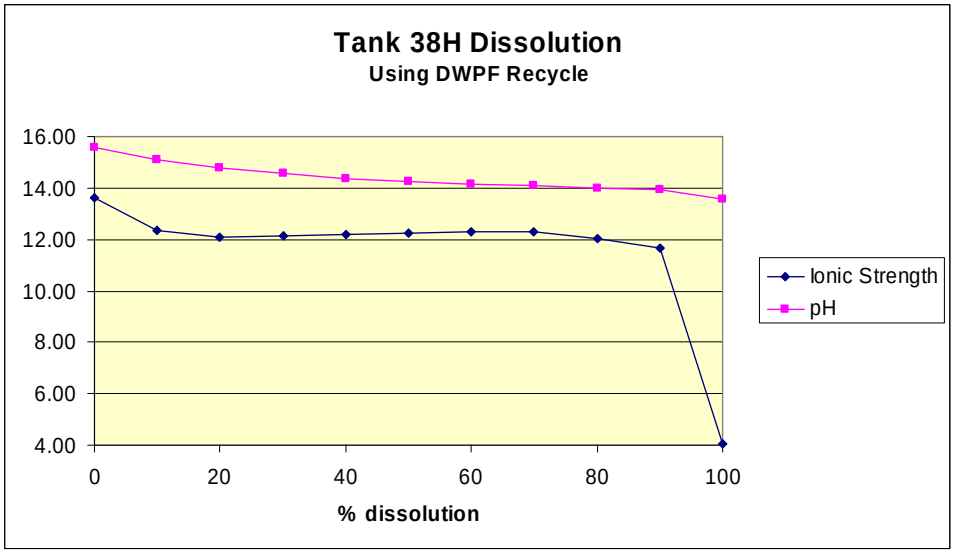

Figure 9 - Tank 38H Transfer Stream Properties

Tank 38H Transfer Stream Corrosion Control

The transfer streams generated by the dissolution process will be collected and stored, for some minimum amount of time, while awaiting further processing by the MST and CSSX technologies. Therefore, it becomes important for these streams to be adjusted to a state that conforms to corrosion control specifications. Figure 10 shows the transfer steams corrosion potential throughout the dissolution process. Above 40% (wt) dissolution, the transfer streams are below acceptable corrosion limits as specified by SRS [7].

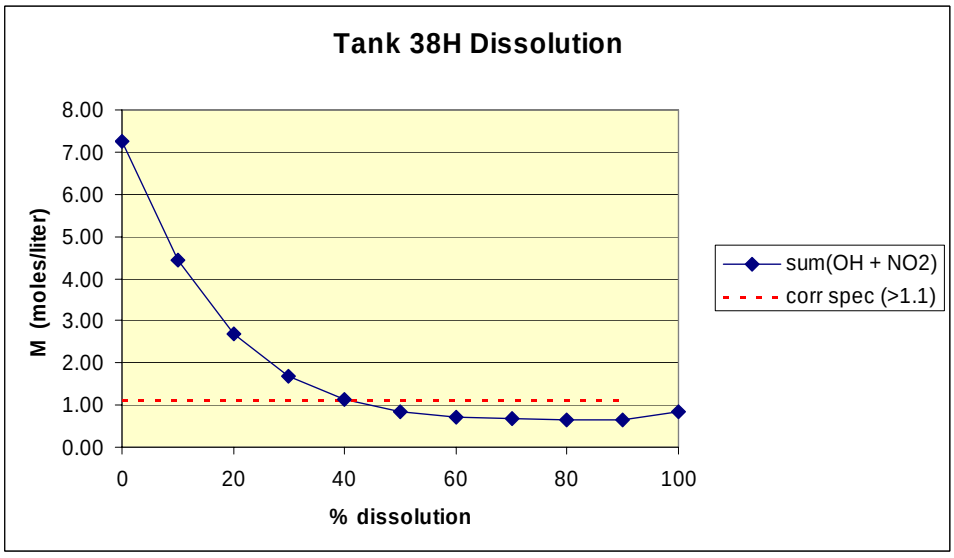

Figure 10 - Transfer Stream Corrosion Potential

Elevation of the OH- and NO2- ion concentrations enough to bring the transfer streams into corrosion compliance may be accomplished by the addition of a stream such as the Batch 5 leachate from sludge processing [4]. The addition of leachate to the dissolution-generated transfer streams was modeled using ESP. As stated before, the dissolution process was modeled for a weight % dissolution from 0 to 100% in increments of 10%. Therefore, the numbering of the transfer streams equates to 1/10 of the % dissolution. For example, transfer stream 1 represents the stream corresponding to 10% by weight of the original tank waste corrected for the free aqueous phase. Figure 11 shows the effect of leachate addition to the various transfer streams. It can be seen that addition of the leachate is effective in reaching corrosion minimum specifications. However, streams from higher dissolutions require up to 20% (volume) to achieve corrosion specifications. Transfer stream 10 is not shown, as it falls under a different corrosion specification because of a lower stream NO_3^- ion concentration. However, the stream 10 results were in corrosion compliance even without leachate addition.

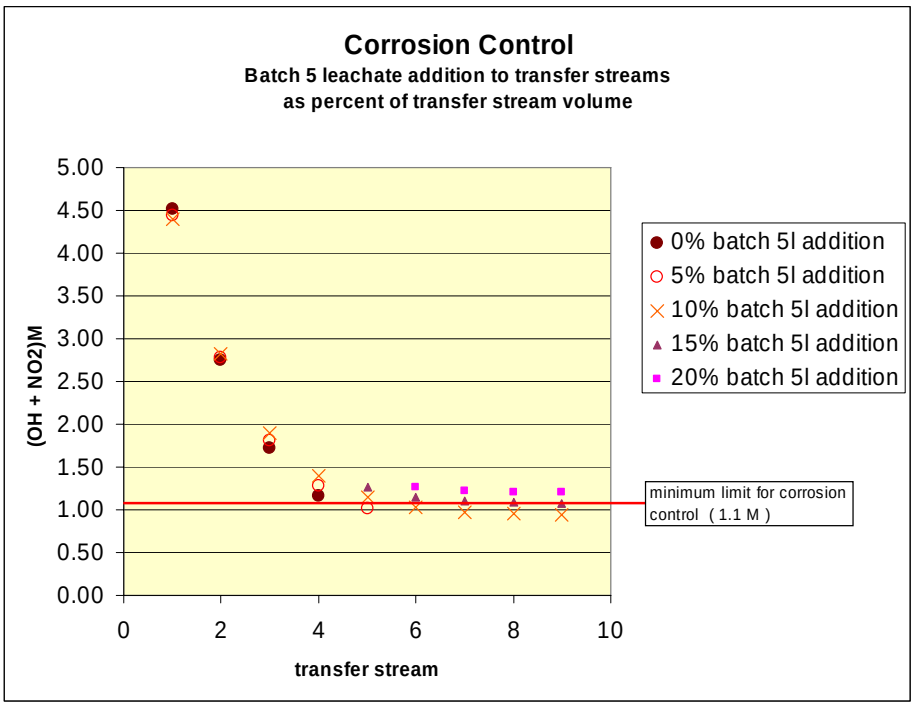

Figure 11 - Corrosion Compliance (with Batch 5 leachate addition)

After the leachate addition, the corrosion compliant transfer stream can be stored in preparation for further processing. Since this will invariably take some time, the ESP simulation modeled the leachate addition and the product stream at 23º C. This was done to predict any solids that might form in the tank from cooling during storage. Figure 12 shows the solids % (wt) after addition of leachate (at 30º C) and cooling to 23º C. Only streams that achieved corrosion compliance are shown. The effect of cooling on solids formation can be seen from the 0% batch addition points. It should also be noted that Batch 5 leachate addition above the amount required to achieve corrosion compliance may be beneficial to reduce the level of solids formation. If the

further addition of leachate to reduce solids is not desired, water can be substituted since most of the solids are nitrates.

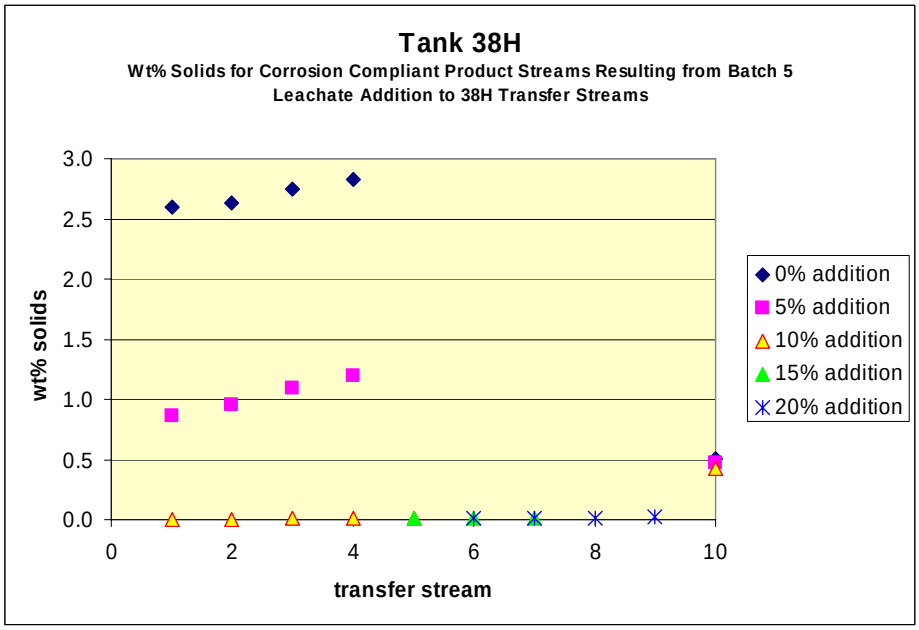

Figure 12 - Transfer Stream Solids (wt% after leachate addition)

CSSX Processing of Tank 38H Tranfer Streams

The CSSX process contacts the waste stream with a specialized organic solvent to remove cesium. Figure 13 represents the portion of the CSSX process that is examined in this report [8]. The organic solvent passes through the extraction and scrub section of CSSX, which is comprised of several in-line centrifugal contactors. The Cs, along with small amounts of tank waste, is removed from the bulk tank waste stream in the extraction section. The scrub section uses 0.05M HNO_3 to remove the carryover tank waste while the Cs is transported, with the solvent, into the next section of the process. An ESP model was constructed to evaluate the effect of the tank waste carryover into the scrub section contactors. In particular, the potential for solids precipitation in the scrub contactors was simulated.

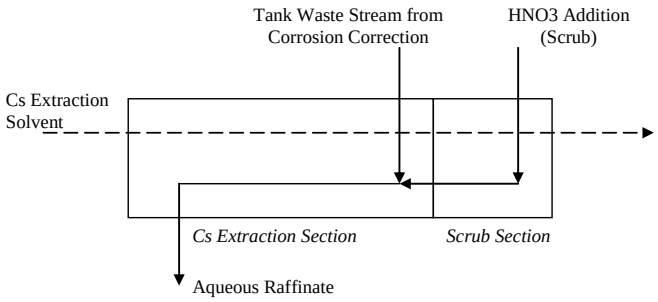

Figure 13 - CSSX (Cs Extraction and Scrub)

The tank waste carryover into the CSSX scrub section was modeled as a percentage, by weight, of the mixture of waste and 0.05M HNO_3 seen in the scrub section contactor. For example, a 1 gram carryover of waste into 99 grams HNO_3 is considered 1% carryover. Carryovers of 1, 3, and 5% (wt) were initially selected for evaluation. Figures 14, 15, 16 and 17 show pH, ionic strength, and total solids (as % by weight) as a function of the transfer stream carryover (also % by weight).

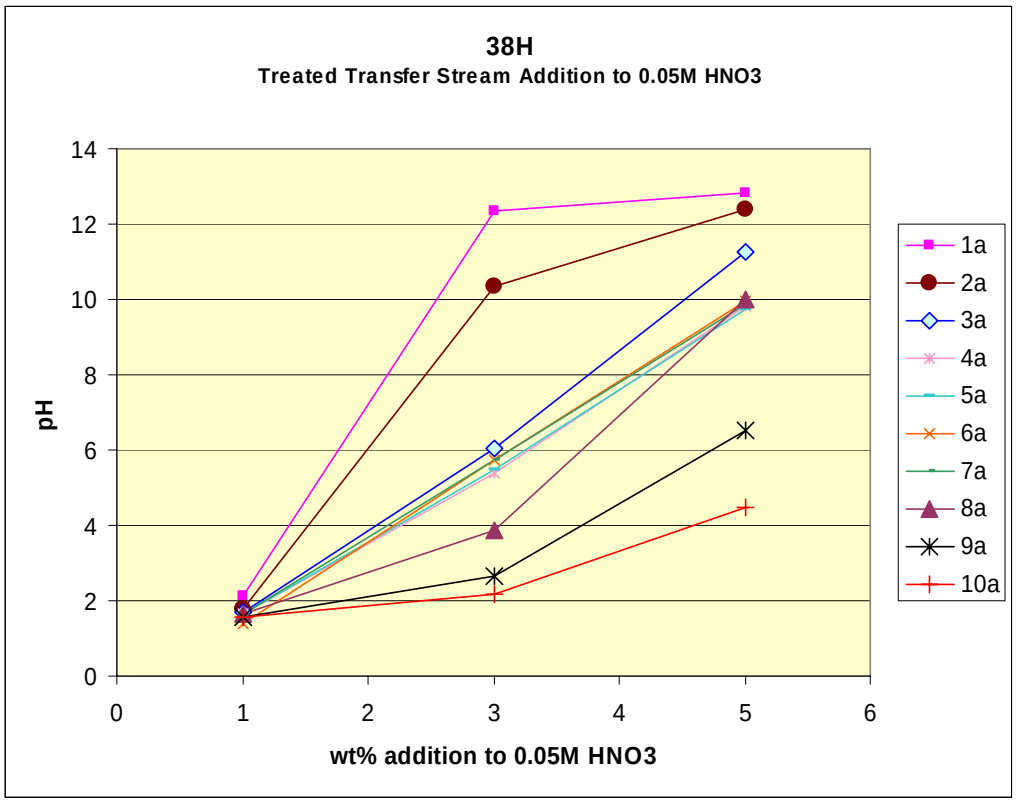

Figure 14 - Effect of Tank Waste Carryover on pH

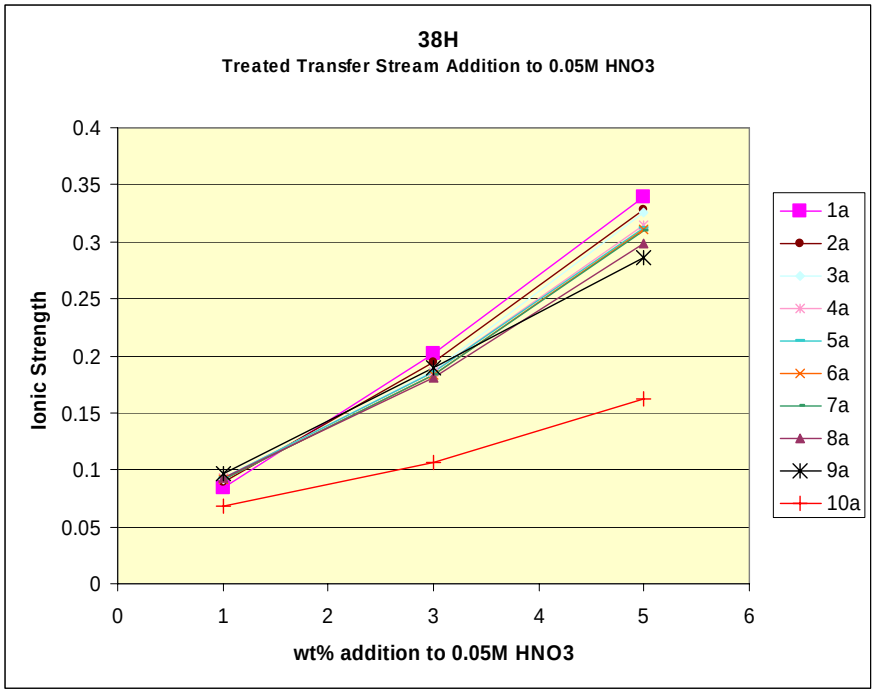

Figure 15 - Effect of Tank Waste Carryover on Ionic Strength

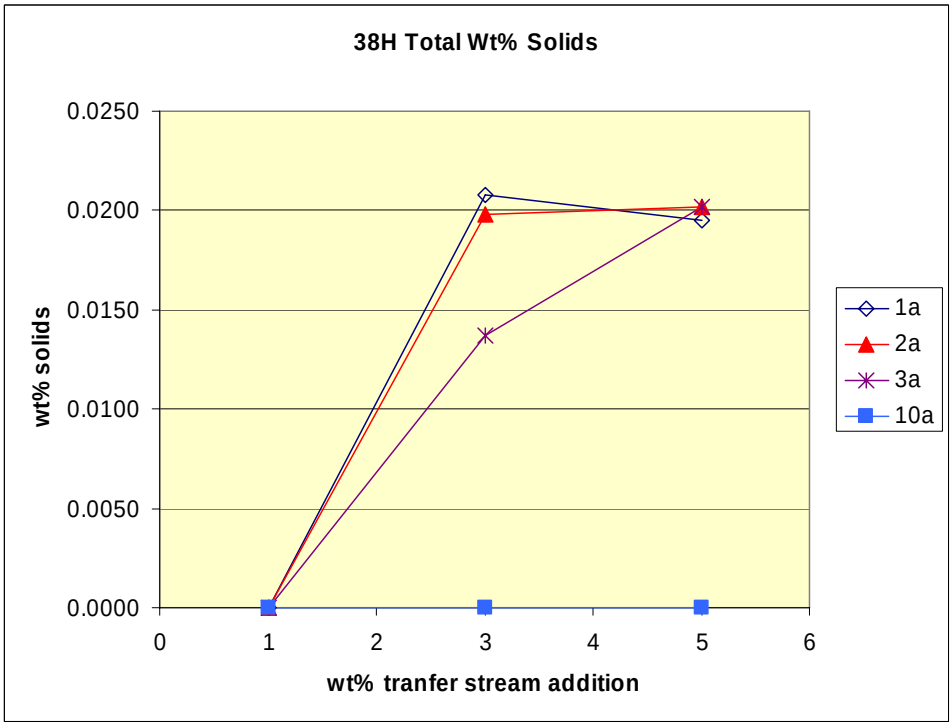

Figure 16 - Effect of Tank Waste Carryover on Wt% Solids

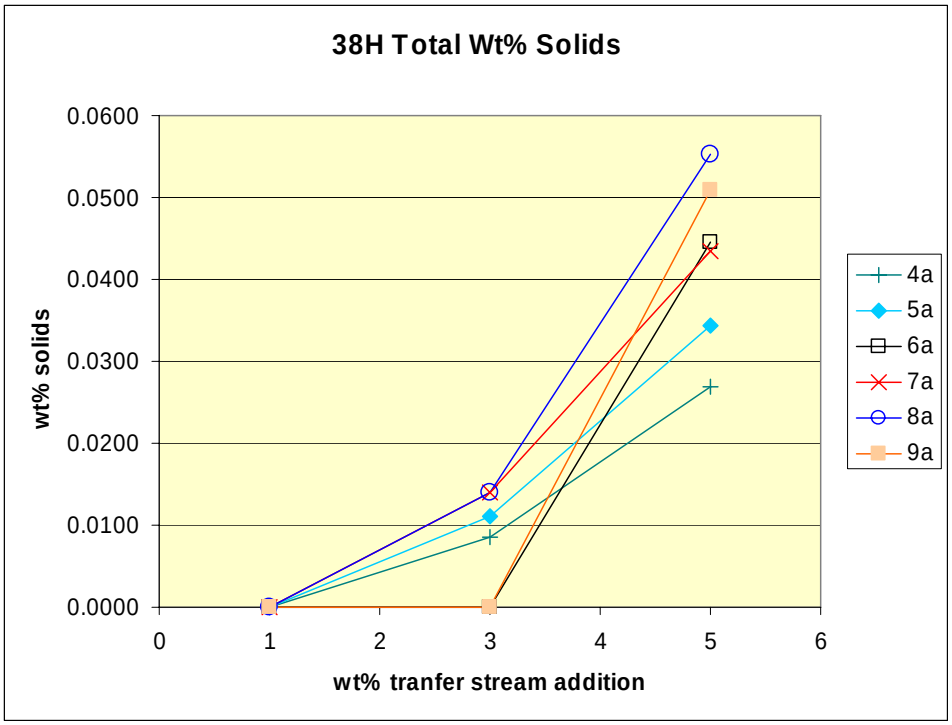

Figure 17 - Effect of Tank Waste Carryover on Wt% Solids

The increase of pH, ionic strength, and weight % solids with an increase of tank waste carryover into the HNO_3 solution is expected. To further evaluate the potential for solids formation from waste carryover into the scrub section, simulation runs were conducted in greater detail for transfer streams 1, 4, and 7. Table 4 summarizes the origin of these streams. Each of these streams was evaluated for carryovers of 1 to 8 % (wt).

Table 4 - Tank 38H Transfer Stream Definitions

Transfer stream	% dissolution	% Leachate addition
1	10	5
4	40	5
7	70	15

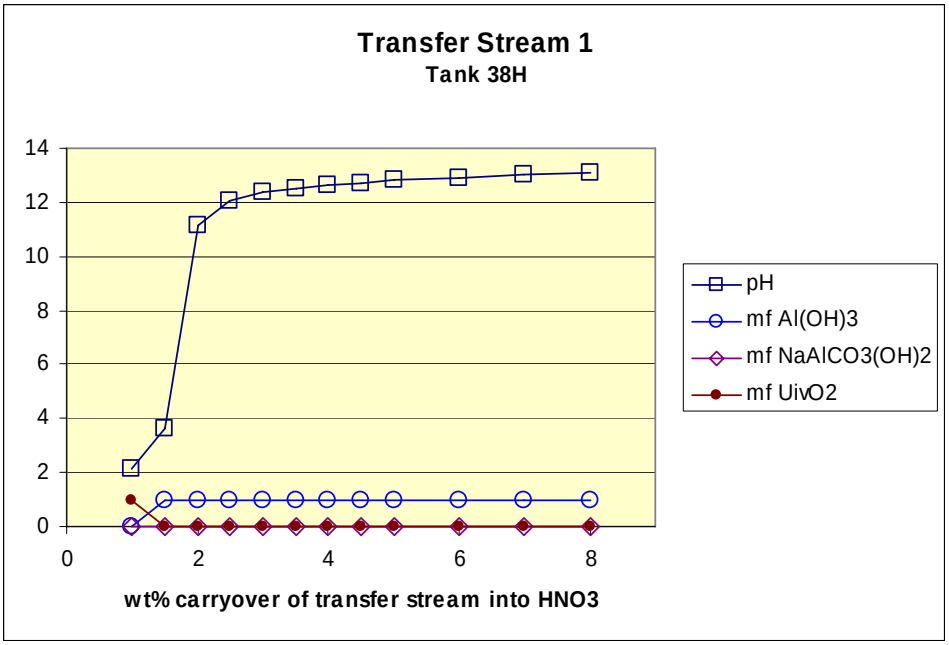

Figure 18 - Transfer Stream 1 Carryover

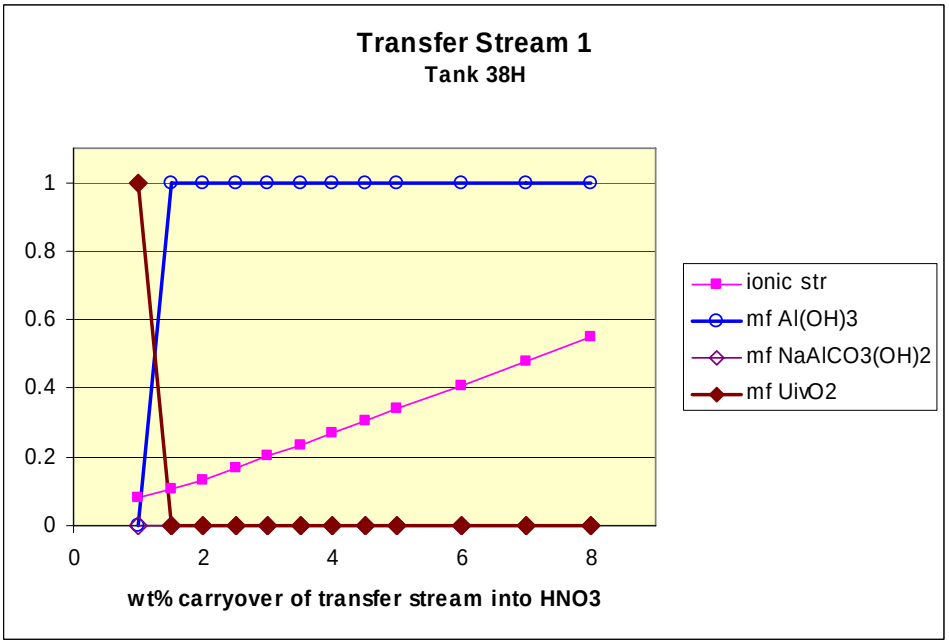

Figure 19 - Transfer Stream 1 Carryover

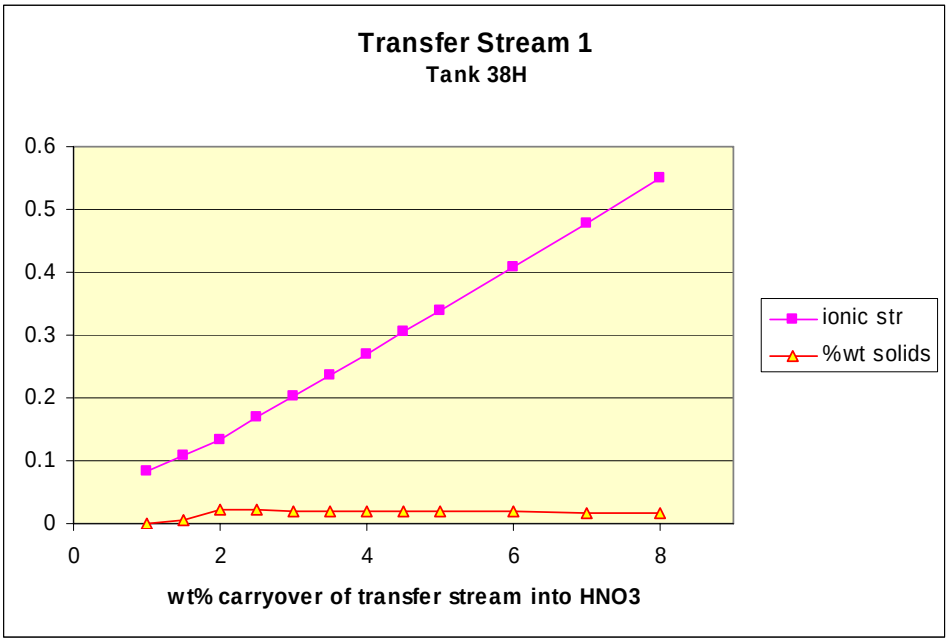

Figure 20 - Transfer Stream 1 Carryover

Figures 18, 19 and 20 show the effect of carryover of transfer stream 1 into the 0.05M HNO3 scrub contactors. At a 1% carryover, the only solid formed is UO_2, although the total amount is effectively zero. At carryover values above 1%, $Al(OH)_3$ becomes the exclusive solid component with a total % solids (wt) of approximately 0.02. The total amount of solids predicted to form during CSSX processing of the entire transfer stream is given in Table 5.

Table 5 - Tank 38H Transfer Stream 1 Predicted Solids Formation

carryover wt%	pH	solids wt%	$Al(OH)_3$ mole fraction	Total $Al(OH)_3$ grams	$NaAlCO_3(OH)_2$ mole fraction	$NaAlCO_3(OH)_2$ total grams	$UivO_2$ mole fraction	$UivO_2$ total grams
1	2.12	5.79E-08	0	0	0	0	1	0.000037
1.5	3.64	4.67E-03	0.999994	2,975	0	0	0.000006	0.061069
1.65	3.88	1.45E-02	0.999998	9,244	0	0	0.000002	0.000000
1.75	4.57	1.80E-02	0.999998	11,516	0	0	0.000002	0.000000
1.85	7.10	2.00E-02	0.999998	12,788	0	0	0.000002	0.000000
2	11.14	2.09E-02	0.999999	13,403	0	0	0.000001	0.040636
2.5	12.08	2.09E-02	0.999394	13,463	0	0	0	0
3	12.35	2.08E-02	0.999243	13,441	0	0	0	0
3.5	12.52	2.06E-02	0.999104	13,368	0	0	0	0
4	12.64	2.03E-02	0.998966	13,250	0	0	0	0
4.5	12.73	1.99E-02	0.998825	13,086	0	0	0	0
5	12.81	1.95E-02	0.998679	12,880	0	0	0	0
6	12.93	1.85E-02	0.998367	12,338	0	0	0	0
7	13.02	1.73E-02	0.998017	11,628	0	0	0	0
8	13.10	1.58E-02	0.997607	10,750	0	0	0	0

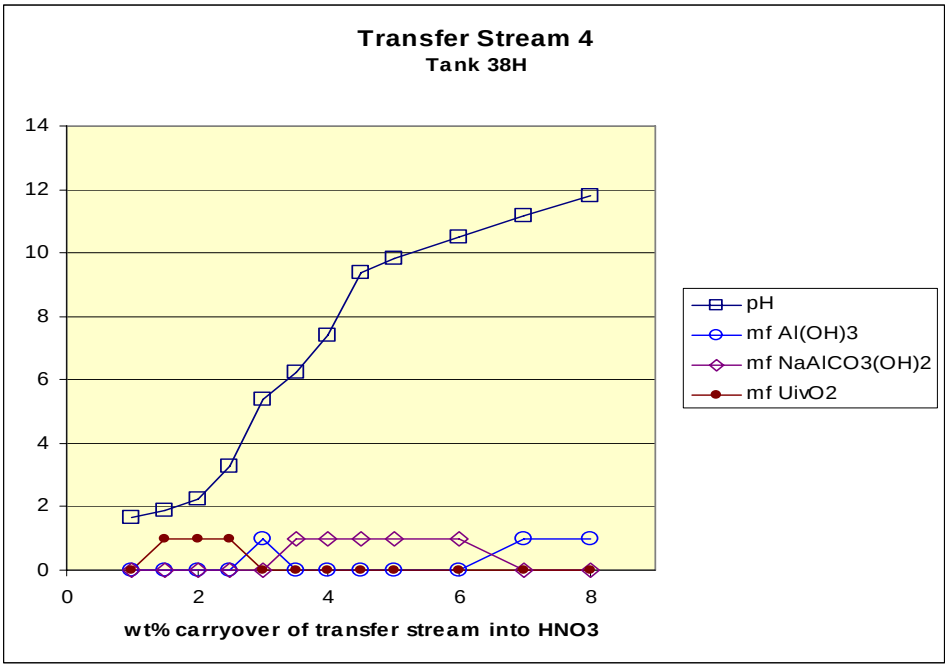

Figure 21 - Transfer Stream 4 Carryover

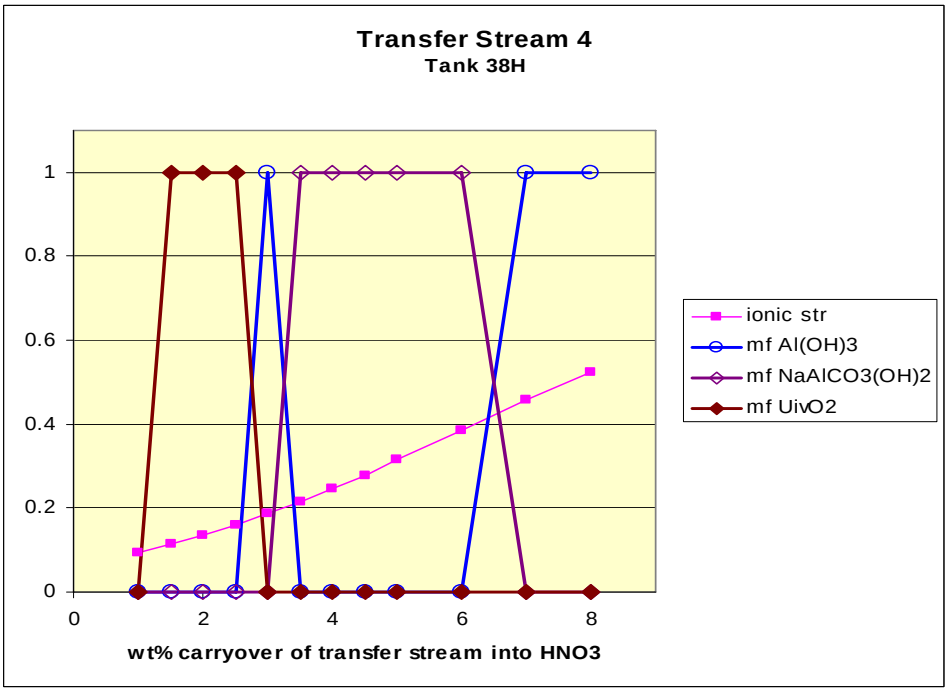

Figure 22 - Transfer Stream 4 Carryover

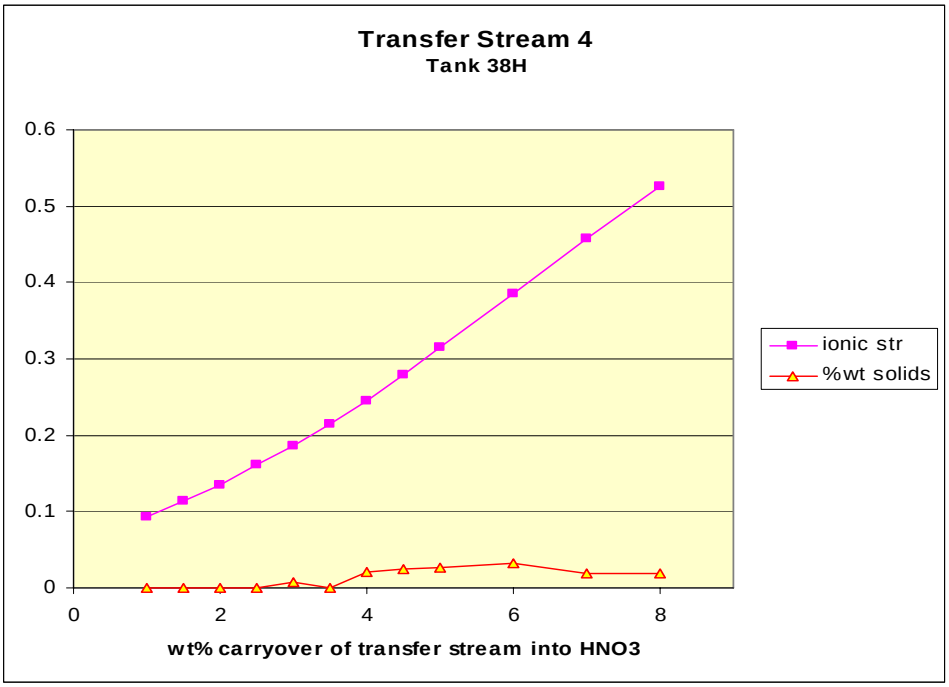

Figure 23 - Transfer Stream 4 Carryover

Figures 21, 22 and 23 show the effect of carryover of transfer stream 4 into the 0.05M HNO_3 scrub contactors. At carryover values of 2.5% or less, the only solid formed is UO_2, although the total amount is effectively zero. At a carryover value of 3%, $Al(OH)_3$ is the predicted solid. Above 3%, NaAlCO3$(OH)_2$ becomes the exclusive solid component with a total % solids (wt) of approximately 0.02. When the carryover exceeds 6%, $Al(OH)_3$ again becomes the dominant solid. The total amount of solids predicted to form during CSSX processing of the entire transfer stream is given in Table 6.

Table 6 - Tank 38H Transfer Stream 4 Predicted Solids Formation

carryover wt%	pH	solids wt%	$Al(OH)_3$ mole fraction	Total $Al(OH)_3$ grams	$NaAlCO_3(OH)_2$ mole fraction	$NaAlCO_3(OH)_2$ total grams	$UivO_2$ mole fraction	$UivO_2$ total grams
1	1.65	0	0	0	0	0	0	0.000000
1.5	1.87	1.10E-07	0	0	0	0	1.000000	0.072789
2	2.25	2.75E-07	0	0	0	0	1.000000	0.182283
2.5	3.29	3.54E-07	0	0	0	0	1.000000	0.235840
3	5.39	8.51E-03	0.999986	5,764	0	0	0.000014	0.285594
3.5	6.26	0	0	0	0.999985	6,970	0.000014	0.335816
4	7.38	2.16E-02	0	0	0.999978	8,008	0.000014	0.386552
4.5	9.40	2.43E-02	0	0	0.999976	9,054	0.000014	0.436953
5	9.83	2.70E-02	0	0	0.999976	10,108	0.000014	0.487197
6	10.51	3.22E-02	0	0	0.999977	12,182	0.000014	0.582875
7	11.18	1.97E-02	0.999967	0	0	0	0.000014	0.644846
8	11.81	1.98E-02	0.997772	0	0	0	0.000012	0.557833

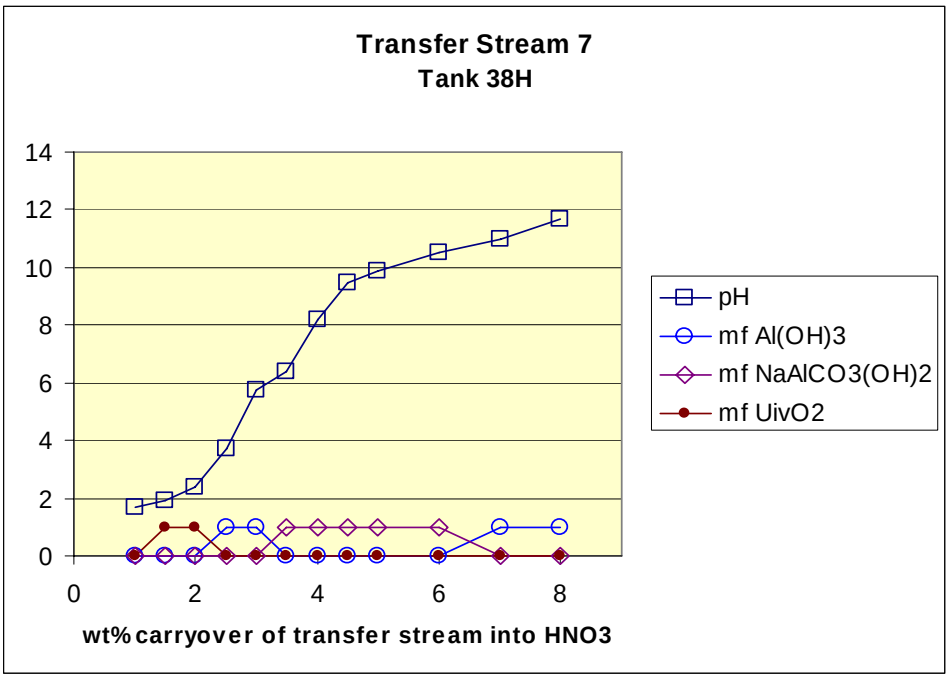

Figure 24 - Transfer Stream 7 Carryover

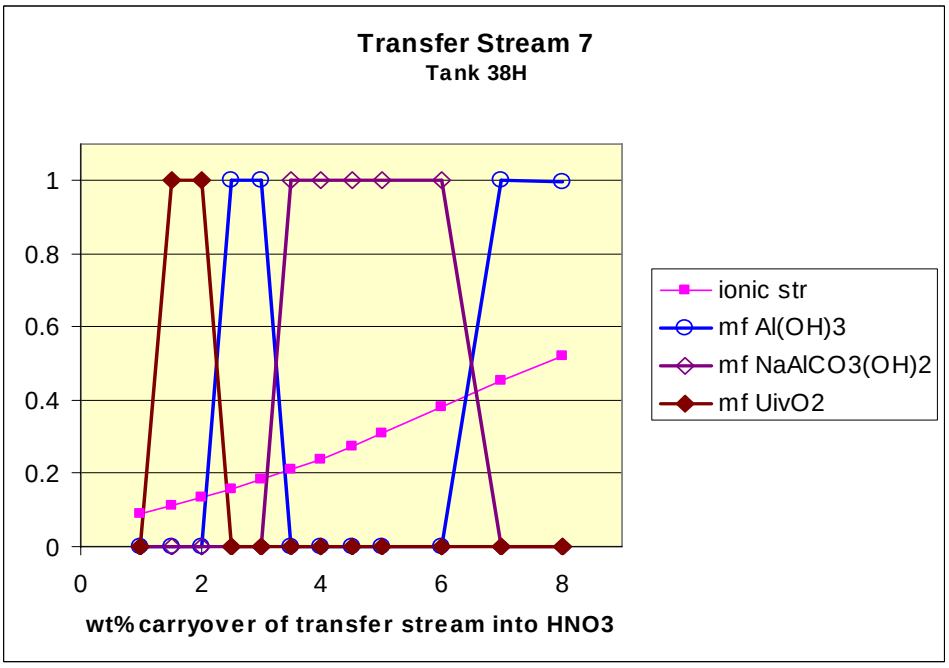

Figure 25 - Transfer Stream 7 Carryover

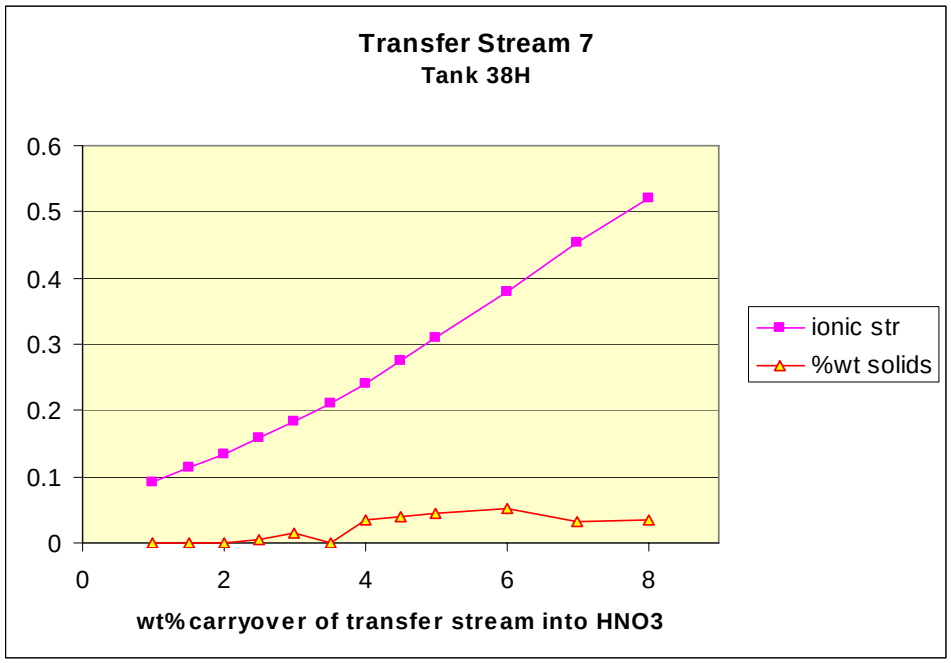

Figure 26 - Transfer Stream 7 Carryover

Figures 24, 25 and 26 show the effect of carryover of transfer stream 7 into the 0.05M HNO_3 scrub contactors. At carryover values of 2.0% or less, the only solid formed is UO2, although the total amount is effectively zero. At carryover values of 2.5 or 3%, $Al(OH)_3$ is the predicted solid. Above 3%, $NaAlCO_3(OH)_2$ becomes the exclusive solid component with a total % solids (wt) of approximately 0.04. When the carryover exceeds 6%, $Al(OH)_3$ again becomes the predicted solid. The total amount of solids predicted to form during CSSX processing of the entire stream is given in Table 7.

Table 7 - Tank 38H Transfer Stream 7 Predicted Solids Formation

carryover wt%	pH	solids wt%	$Al(OH)_3$ mole fraction	Total $Al(OH)_3$ grams	$NaAlCO_3(OH)_2$ mole fraction	$NaAlCO_3(OH)_2$ total grams	$UivO_2$ mole fraction	$UivO_2$ total grams
1	1.67	0	0	0	0	0	0	0
1.5	1.90	1.34E-07	0	0	0	0	1.000000	0.097771
2	2.36	2.71E-07	0	0	0	0	1.000000	0.198987
2.5	3.74	3.82E-03	0.999974	2,847	0	0	0.000026	0.254094
3	5.74	1.41E-02	0.999991	10,535	0	0	0.000009	0.307691
3.5	6.42	0.E+00	0	0	0.999991	12,413	0.000009	0.361823
4	8.22	3.48E-02	0	0	0.999986	14,261	0.000009	0.416457
4.5	9.48	3.91E-02	0	0	0.999985	16,124	0.000009	0.470590
5	9.87	4.34E-02	0	0	0.999985	18,004	0.000009	0.524657
6	10.51	5.19E-02	0	0	0.999975	21,754	0.000008	0.627664
7	10.95	3.25E-02	0.999957	25,372	0	0	0.000008	0.718985
8	11.69	3.51E-02	0.996647	27,612	0	0	0.000007	0.665311

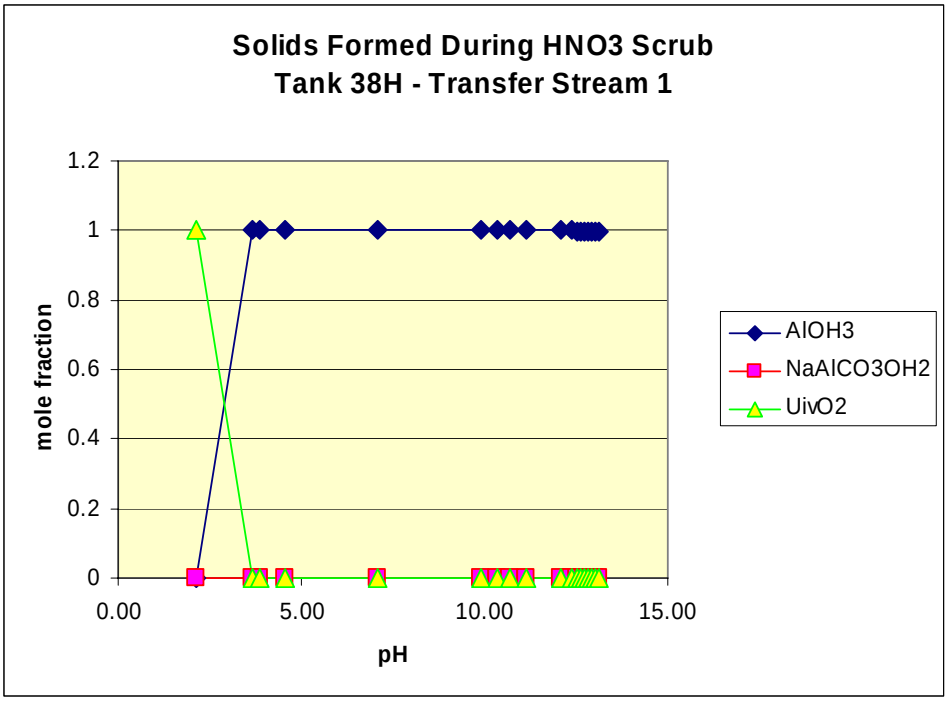

Figure 27 – Predicted Solids Formation for Transfer Stream 1

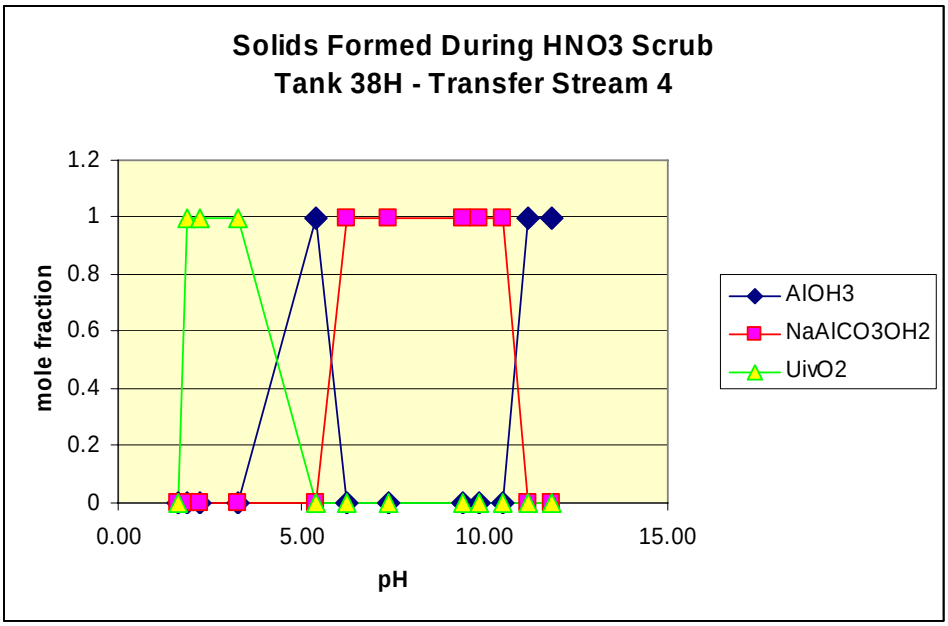

Figure 28 – Predicted Solids Formation for Transfer Stream 4

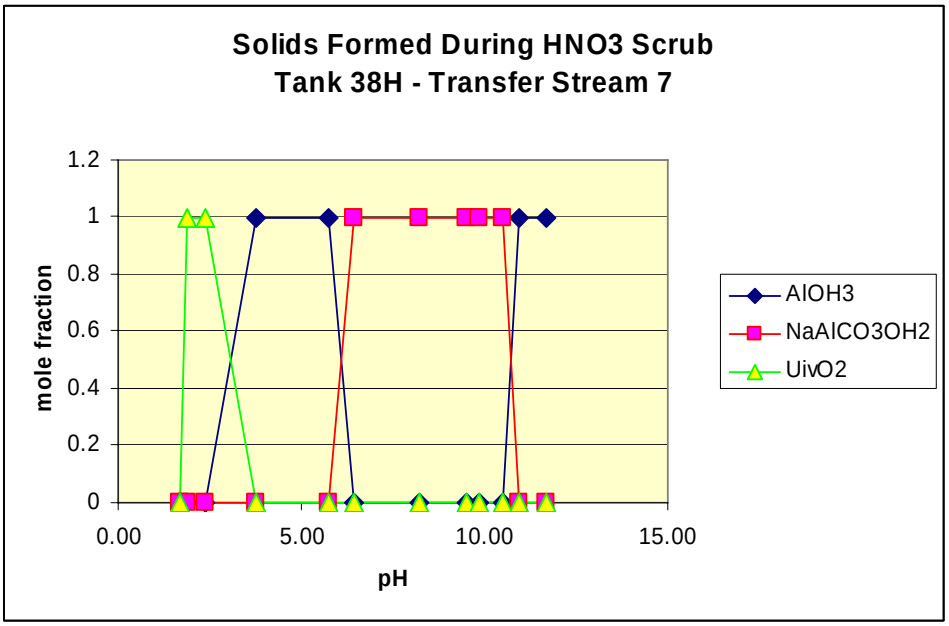

Figure 29 – Predicted Solids Formation for Transfer Stream 7

A comparison of the predicted solids for tank waste streams 1, 4 and 7 is shown in Figures 27, 28 and 29. In these plots, the mole fraction of solid components is shown versus the resulting pH of the HNO_3 stream containing tank waste carryover. Figure 27 shows that for carryover of transfer stream 1, $Al(OH)_3$ is the only solids predicted when the mix stream pH is above approximately 3. However, for carryover of transfer streams 4 and 7 into the HNO_3 scrub contactor, as shown in Figures 28 and 29, the appearance of $Al(OH)_3$ above a pH of 3 is followed by a change to $NaAlCO_3(OH)_2$ in the pH range of approximately 6 to 10.5. Above a pH of 10.5, $Al(OH)_3$ again becomes the predicted solid.

Table 8 - CSSX Aqueous Raffinate

	Aqueous Raffinate		
Transfer Stream	pH	ionic str.	total solids wt%
1	15.2	10.3	0.000000
4	14.4	10.0	0.000002
7	14.3	9.8	0.000004

As shown in Figure 13, the tank waste stream (minus the extracted Cs) and the HNO_3 scrub stream ultimately combine and leave the CSSX process as Aqueous Raffinate. A check of this

final combined stream is given in Table 8. As seen from this data, the predicted total solids loading is essentially zero.

CONCLUSIONS

The results from ESP simulation of SRS Tank 38H indicate that DWPF recycle can be used to recover the saltcake in place of caustic water. As expected from the high level of nitrate in the initial saltcake solids, the Na, OH, NO_3^-, and NO_2^- ions dominate most of the dissolution. As 100 % (wt) dissolution is approached, $Na_2C_2O_4$ replaces $NaNO_3$ as the major remaining solid and at 100 % (wt) dissolution, no $NaNO_3$ remains in the saltcake. An evaluation of dissolution transfer streams as per adherence to corrosion specifications show that corrosion compliance is maintained for dissolutions below 40 % (wt). The addition of Batch 5 leachate to streams above 40 % dissolution was effective in reaching corrosion minimum specifications. However, streams from higher dissolutions require up to 20% (volume) leachate to achieve corrosion specifications. Simulation of dissolution stream cooling during storage predicted that solids precipitation would occur in streams that were not treated with leachate addition.

Simulation of carryover of dissolution stream into CSSX scrub section contactors was conducted to predict the potential for solids precipitation, which could lead to contactor fouling. At 10% dissolution, 0.02 % (wt) solids, $Al(OH)_3$, is predicted for pH values above 3. For higher dissolution streams approximately 0.04 % (wt) solids are predicted above a pH of 3. However, $NaAlCO_3(OH)_2$ is indicated as the only solid between pH values of 6 and 10.5. At all other pH values, above 3, $Al(OH)_3$ is the only predicted solid. At pH values below 3, essentially zero solids precipitation, 10^{-7} % (wt) solids, was indicated.

WORK PLANNED FOR NEXT QUARTER

During the 2nd quarter of 2009, simulations will be conducted for SRS Tank 31H.

REFERENCES

1. Baitch, M. A. et al., " Sludge Batch 4 Simulant Flowsheet Studies with ARP and MCU: Impact of MCU Organics," WSRC TR-2005-00230, Rev.0, Savannah River National Laboratory, Aiken SC, 2005.
2. Wusu, K. A., Walker, D. D. and T. B. Edwards, " Solvent Composition Limits for Modular Caustic-Side Solvent Extraction Unit (MCU)," WSRC TR-2005-00258, Rev.0, Savannah River National Laboratory, Aiken SC, 2005.
3. Lindner, J. S., Smith, L. T., Antonyraj, A. and R. K. Toghiani, "Thermodynamic Simulations in Support of Savannah River Site Tank 41H Retrieval and Processing," Letter Report, July 2003.
4. Lindner, J. S., Smith, L. T. " Modeling and Experimental Support for High Level SRS Salt Disposition Alternatives," in Accelerating Cleanup of the Defense Nuclear

Legacy, Report No.07040R02, Institute for Clean Energy Technology, Mississippi State University, 2008, OND.
5. Martino, C. J., Nichols, R. L., McCabe, D. J., Hansen, E. K., “Tank 38H Saltcake Core and Supernate Sample Analysis”, WSRC-TR-2004-00129, Rev 0, Westinghouse, Savannah River Company, Aiken SC (2004).
6. Shah, S. C., Hopkins, M. D., “Curie Calculation Basis for Salt Strategies”, correspondence to Renee Spires, Westinghouse, Savannah River Company, Aiken SC, 24 Feb 2004.
7. Tank Farm Corrosion Control Program, WSRC-IM-2003-00010, Rev. 3.
8. Birdwell, J. F. et al., “Conceptual Design of a Simplified Skid-Mounted Caustic-Side Solvent Extraction Process for Removal of Cesium from Savannah River Site High-Level Waste”, ORNL/TM-2004/59, May 2004.

Task 1.2: SRS Saltstone Process Studies

Ronald A. Palmer, W. P. Okhuysen, R. Arunkumar

INTRODUCTION

This project is designed to assist the Savannah River National Laboratory (SRNL) in the production of the Saltstone waste form from low-level waste. The expectation of increased aluminum content in the next batch has raised concerns about an excess heat of hydration that may create problems for the storage of the waste form. The facility also relies on vault temperature modeling to protect vault temperature limits. These studies are designed to examine the effects of the heat created by the reactions and to discover methods for either dealing with the excess heat or preventing it from occurring in the first place.

The basic design for the adiabatic calorimeter is taken from the work of Steimke and Fowley [1]. This document provides the general outline of operation of the instrument, properties of the then-current Saltstone formulation, and expected performance of the instrument. References from Harbour [2-3] provide information on the properties of both the raw materials and the Saltstone itself.

This device will provide basic thermal property measurements (heat of hydration in particular). These data are important contributions to new revisions of the Performance Assessment documentation.

This project is comprised of two subtasks. The first consists of laboratory scale (sample sizes of about one liter) experiments designed to examine the thermal properties of new Saltstone formulations. The second consists of pilot scale studies of 55-gallon drum sized samples.

Laboratory Scale Experiments

Small batches prepared in the laboratory must be done prior to designing the pilot scale tests. Laboratory methods are being set up for preparing the simulated salt solution, mixing the waste form, and measuring the heat of hydration for various Saltstone formulations.

Pilot Scale Studies

Small batches prepared in the laboratory can only provide preliminary information. A pilot-scale facility, capable of producing 55-gallon drum sized product, is available at the ICET laboratories. Drums can be appropriately instrumented to examine the heat generation of Saltstone formulations on an intermediate scale between the laboratory and actual Saltstone production facility.

Using these same waste simulant recipes, various formulations of Saltstone will be produced at our pilot-scale facility. The laboratory scale work provides the basis for determining which formulations to study further. The results of this work will provide the confidence necessary for full scale production at the Saltstone production facility. Lee [4] and Cozzi, et al. [5] have done similar work at SRNL. The design of experiments done for this project will be based on their work on other cement waste forms.

WORK ACCOMPLISHED DURING THIS QUARTER

During this quarter, the construction of the adiabatic calorimeter was completed and a series of initial experiments to study the behavior of the instrument and to get a sense of how the materials react in the experiments was performed.

INSTRUMENT DESIGN AND CONSTRUCTION

Based on the article by Steimke and Fowley and conversations with our colleagues at SRNL, we designed and built an adiabatic calorimeter. Figure 30 is a block diagram of the instrument itself; Figure 31 is a block diagram of the wiring diagram for the thermocouples, stirrer, heater, and various other equipment associated with the calorimeter.

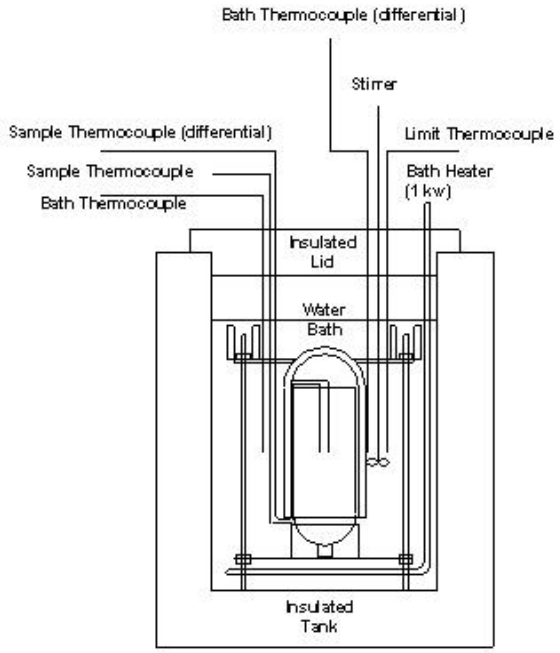

Figure 30 Adiabatic Calorimeter

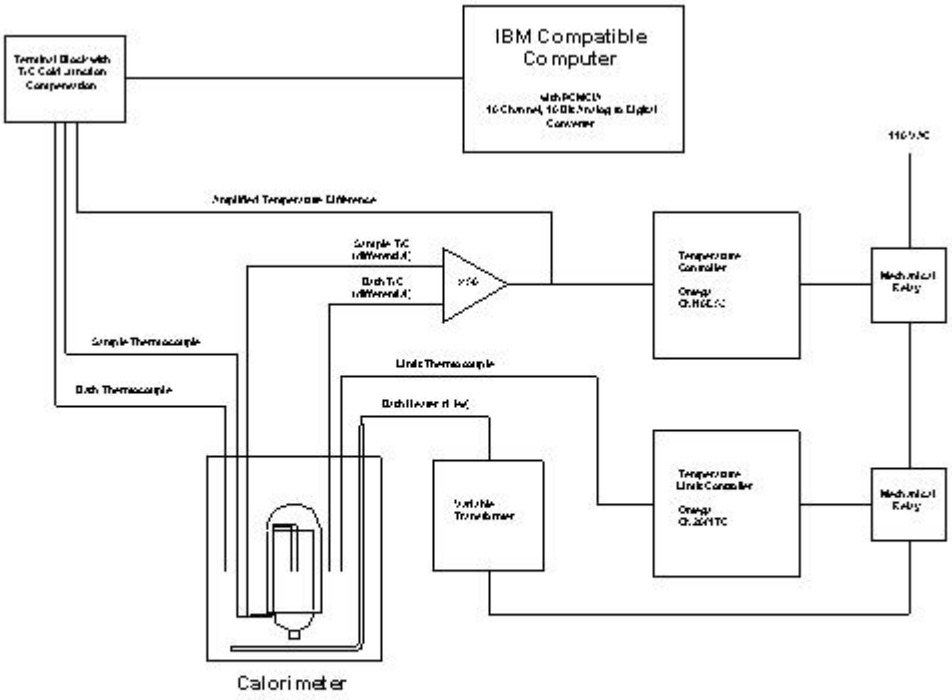

Figure 31 Adiabatic Calorimeter

The materials employed are reagent grade chemicals and raw materials that were available in these laboratories from previous projects. Table 9 shows the reference salt solution recipe as taken from Steimke and Fowley. The same article provided the reference Saltstone recipe shown in Table 10.

Table 9. Reference Salt Solution Recipe	
Compound	**Grams/Liter**
100% by Weight NaOH	114.64
$NaNO_3$	167.66
$NaNO_2$	33.43
Na_2CO_3	12.46
Na_2SO_4	7.84
Aluminum Nitrate (9 H_2O)	42.90
Sodium Phosphate (1 H_2O)	1.00
Total Salt mass	303.51

Table 10. Reference Saltstone Recipe	
Compound	Wt %
Salt solution	46.0
Portland Cement	6.0
Blast Furnace Slag	24.0
Fly Ash	24.0

Figure 32 shows the results of an experiment with Type II Portland Cement and water. Without the dilution effects of fly ash and slag, the final temperature exceeds 100C. Because the water in the bath began to boil, we essentially lose control of the experiment at that point.

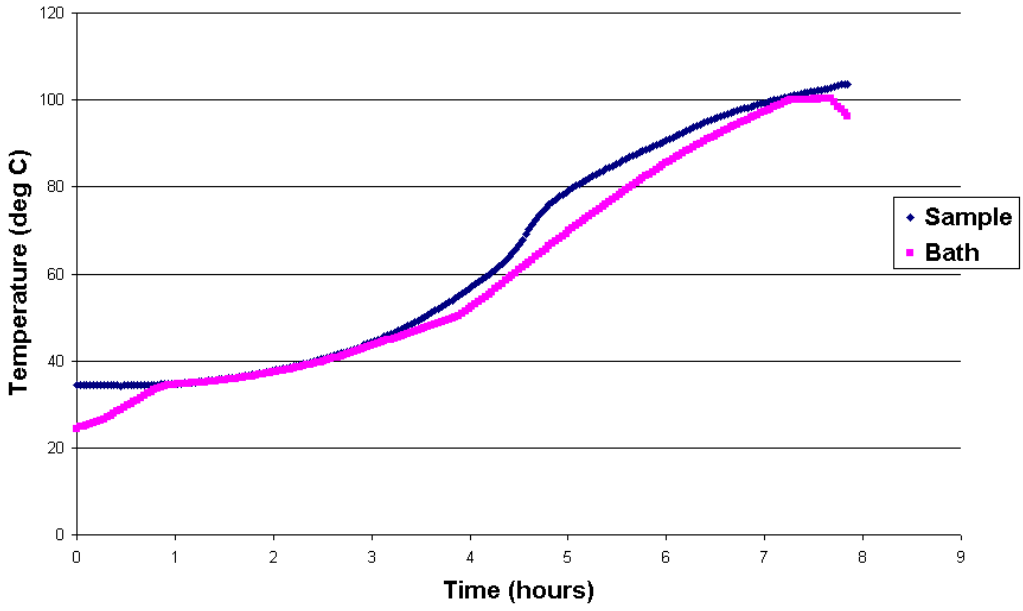

Figure 32. Type II Portland Cement with water.

Figure 33 shows the results of an experiment testing the Reference Saltstone formulation with water. The temperatures of the sample and the bath track each other more closely in this experiment.

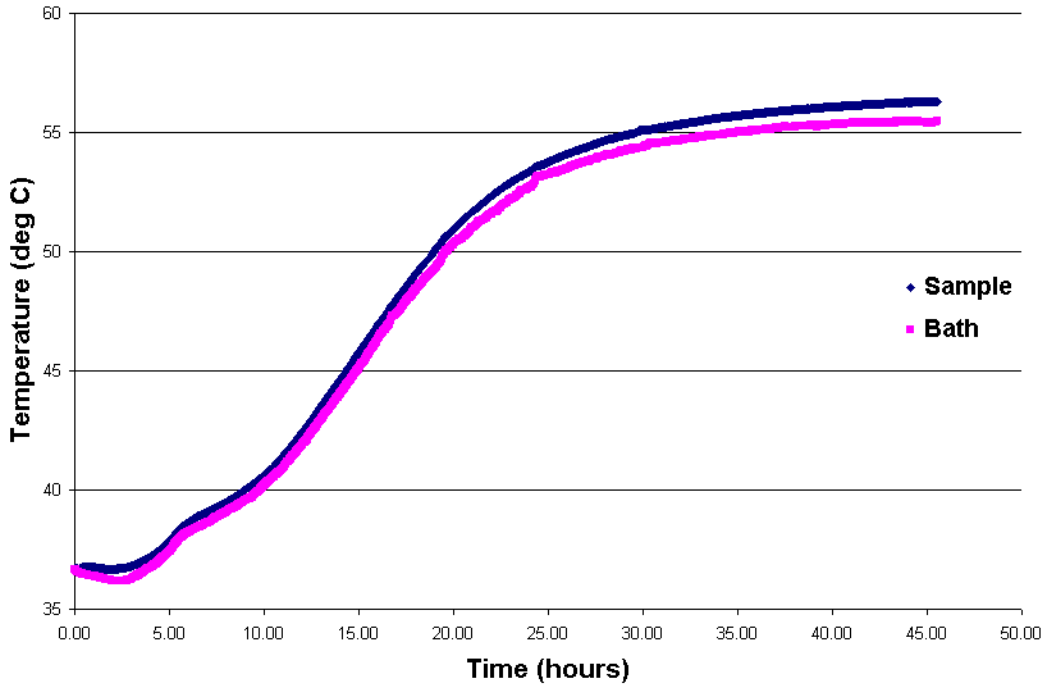

Figure 33. Reference Saltstone formulation with water.

Figure 34 compares two runs with the Reference Saltstone formulation plus salt solution. Run 1 had a duration of about three days whereas Run 2 extended over 12 days. This was the first of a series of runs that will be performed specifically to examine the reproducibility of the instrument.

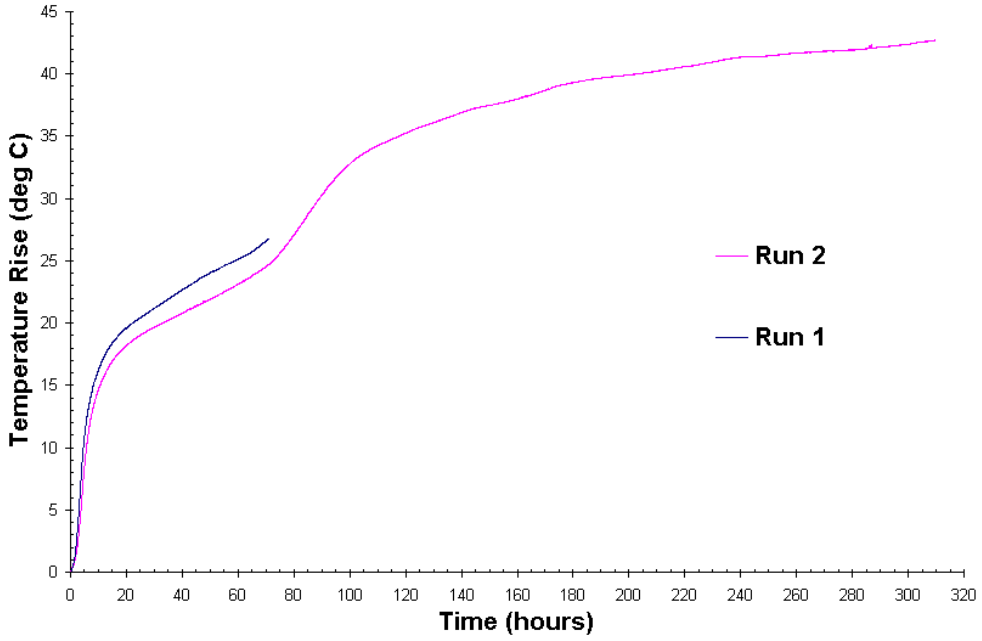

Figure 34. Reference Saltstone formulation plus salt solution (Runs 1 and 2).

Figure 35 shows the end of a run with the Reference Saltstone formulation plus salt solution**.** At about 287 hours, the amplifier used for controlling the calorimeter bath temperature was upgraded. About three hours later, the temperature controller set point was adjusted. The changes resulted in much better tracking of the sample temperature by the bath temperature, within about 0.05C. Options are being addressed to achieve better instrument performance.

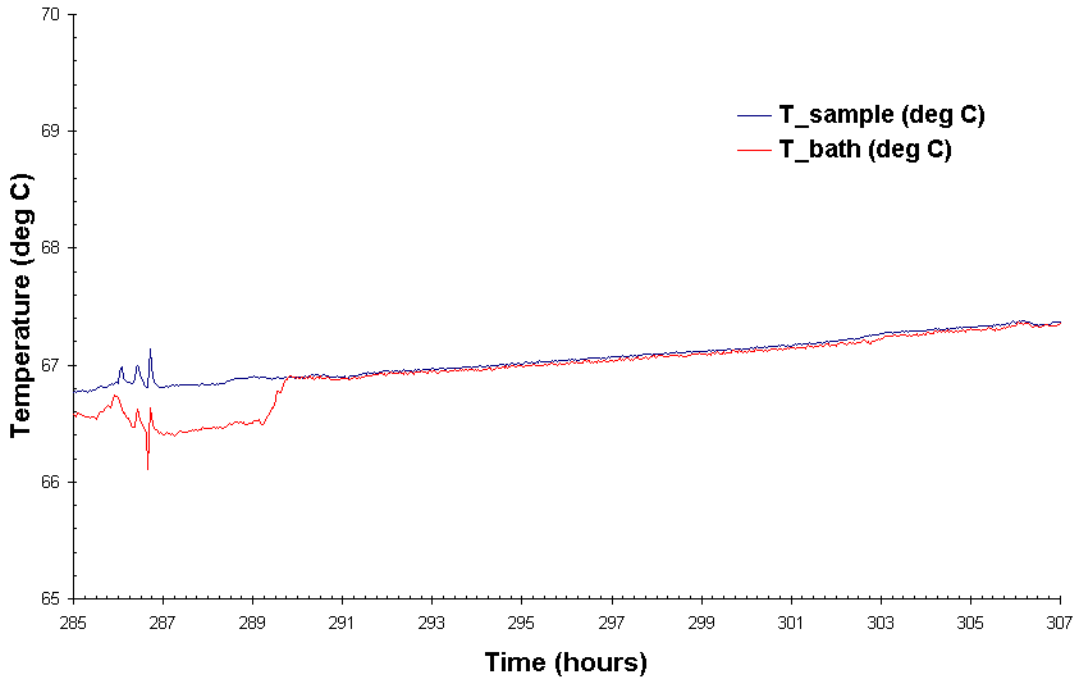

Figure 35. Reference Saltstone formulation plus salt solution**.**

The instrument currently is placed in the high bay; and moving the system to the prep lab is expected soon to make way for additional work in the high bay. Other work in the laboratory during this reporting period included:

- Designing experiments with 1kg batches studying the heat evolution of the Saltstone formulations using containers outfitted with thermocouples,
- Continued working toward a test plan due March 31, and
- Investigate the possibility of adding a modeling task to this activity.

CONCLUSIONS

The experiments done during this quarter demonstrate the capabilities of the instrument as well as the identification of some improvements. During the next quarter, similar experiments will be done in order to establish a consistent methodology to provide data and a greater understanding of the instrument as well as the properties of the Saltstone.

WORK PLANNED FOR NEXT QUARTER

The following tasks are expected to be active during the next quarter:

- Continue to experiment with the protocol for making salt solutions and small batches of Saltstone formulations,
- Investigate the possibility of adding a modeling task to this activity,
- Investigate the possibility of using the Differential Scanning Calorimeter for making specific heat measurements, and
- Development of a test plan.

REFERENCES

1. Steimke, J. L. and M. D. Fowley, "Measurement of Thermal Properties of Saltstone," WSRC TR-97-00357, Westinghouse Savannah River Company, Aiken, SC, 1997.
2. Harbour, J. R. et al., "Characterization of Slag, Fly Ash and Portland Cement for Saltstone," WSRC-TR-2006-00067, Revision 0, Savannah River National Laboratory, Aiken, SC, 2006.
3. Harbour, J. R. et al., "Heat of Hydration of Saltstone Mixes – Measurement by Isothermal Calorimetry," WSRC-STI-2007-00263, Revision 0, Savannah River National Laboratory, Aiken, SC, 2007.
4. Lee, Si Young, "Thermal Performance Analysis for WSB Drum," WSRC-STI-2008-00262, Savannah River National Laboratory, Aiken, SC, May 2008.
5. Cozzi, A. D., et al., "Effect of Heat of Hydration on Drum Temperature and Filter Performance in Full-Scale Waste Solidification Building Simulated High Activity Waste Drums," WSRC-STI-2008-00367, Revision 0, Savannah River National Laboratory, Aiken, SC, September 2008.

Process Chemistry Support of Hanford Waste Operations Planning

L. T. Smith, R. K. Toghiani, and J. S. Lindner

Initial aluminum solubility studies for Hanford were performed by Barney [1] Current Hanford pretreatment processing of tank waste with high aluminum content calls for the addition of large amounts of caustic in order to avoid aluminum solids precipitation. The additional caustic increases the sodium content such that it would require significant dilution before ^{137}Cs removal in the ion exchange process. Additionally, the addition of large amounts of sodium will result in the generation of additional low activity waste. This dilution would then affect the aluminum equilibrium. Expanded laboratory studies for aluminum solubilities in the region of these processes and the resulting data would refine and enhance the Barney Diagram currently used for caustic addition estimation.

Extensive solubility studies on sodium salts found within Hanford tank wastes have been performed in these laboratories leading to the creation of the ICET V7DBLSLT database. This database has been incorporated into the MSE platform of the Environmental Simulation Program (ESP, OLI Systems, Inc.) and has lead to improved model predictions for many of the double salts found during processing tank wastes. [2-5]. Recent studies on aluminum in various caustic loadings have shown enhanced solubilities in the presence of sodium nitrate at ambient temperatures. [6] Expanding these studies to include other sodium salts and temperature variations is currently under investigation. Reduction of the amount of caustic used for the waste pretreatment would amount to savings in time and cost for the pretreatment processes involved. In addition, refinement of the original data and expansion by new data due to improved analytical methodology will improve ESP model predictions and enhance the understanding of waste stream chemistries for future downstream processing.

WORK ACCOMPLISHED

Subtask 2.1.1

Laboratory Solubility Test Design

A test plan is proposed to examine the impact of various species on the solubility of gibbsite in solution. Knowledge of enhancement or suppression of gibbsite solubility in the presence of

ions known to be present in the Hanford waste will provide for greater confidence in planning activities and a risk reduction during process operations. The test plan is designed to examine those species present in the waste that are thought to impact aluminum solubility to the largest extent, including sodium nitrate, sodium nitrite and sodium carbonate. Key questions addressed by the test plan include:

- What is the influence of sodium ion on gibbsite solubility?
- What is the influence of hydroxide ion on gibbsite solubility?
- What are the influences of anions (nitrate, nitrite, carbonate, and/or sulfate) on gibbsite solubility?
- How do these influences change as a function of temperature?

Preliminary predictions of gibbsite solubility in solution were performed using ESP V8 and the V7DBLSLT database. It is expected that the results from this experimental plan will eventually be incorporated into the MSE database and will serve to improve ESP predictions of gibbsite solubility for process design and waste treatment planning activities at Hanford.

Shown in Figures 36 and 37 are preliminary predictions of gibbsite solubility for the temperature range of 25 to 60 °C. Experimental solubility data of Szita and Berecz as taken from Apps et al (1988) [7] are also included in the figures. The data of Russell et al. at 40 °C and 60 °C are also included in Figure 37. At the lowest temperature (25 °C), ESP predictions are in excellent agreement with the experimental data over the sodium molality range. However, at 50 and 60 °C, the predictions are slightly lower than the experimental data, with a greater difference observed for the lower end of the sodium molality range.

Predictions were also performed to examine the impact of sodium nitrate on the gibbsite solubility. Shown in Figures 38 and 39 are the predictions at 25 °C. In Figure 38, the horizontal axis is sodium in solution (m), while in Figure 39, the horizontal axis is free hydroxide in solution. The presence of sodium nitrate in solution at 1m concentration essentially shifts the curve along the sodium axis, but when the data are plotted using free hydroxide along the horizontal axis, the predictions fundamentally fall on the same curve. There is no significant difference in the predicted gibbsite solubility in the presence of 1m sodium nitrate in solution versus no sodium nitrate. Unpublished experimental measurements in our laboratory for gibbsite solubility in 1 and 3 m caustic at 25 °C with varying levels of sodium nitrate are shown in Figure 40. These data further demonstrate that the presence of sodium nitrate alone in caustic solution does not significantly change the aluminum in solution. These experiments were performed using aluminum wire as the source for aluminum, and solids from each sample were identified as gibbsite and/or sodium nitrate.

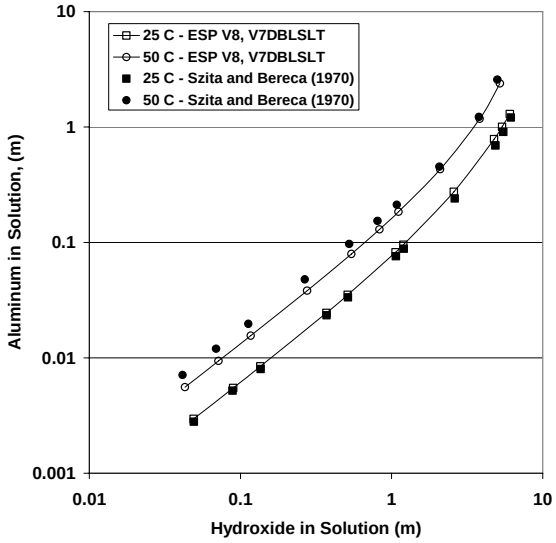

Figure 36. Comparison of ESP Predictions at 25 and 50 °C to the Experimental Data of Szita and Bereca (taken from Apps et al., 1988).

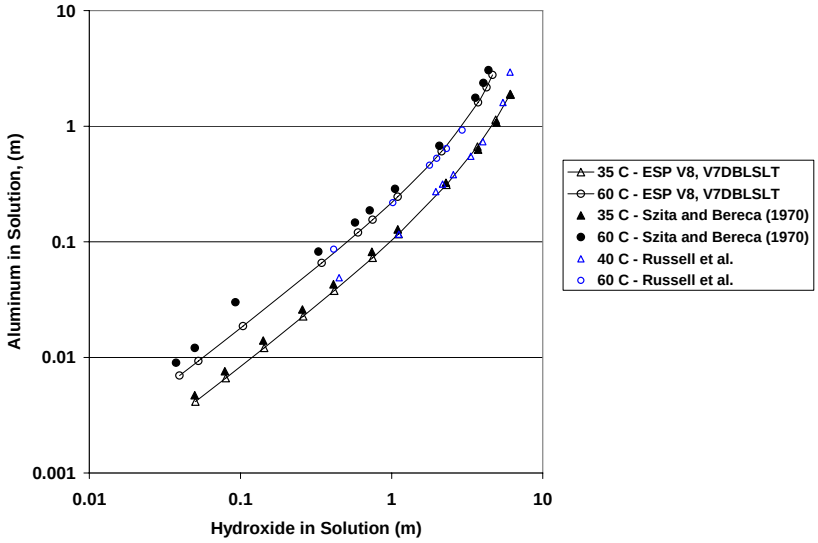

Figure 37. Comparison of ESP Predictions at 35 and 60 °C to the Experimental Data of Szita and Berecz (taken from Apps et al., 1988) and to the Experimental Data of Russell et al. (taken from Apps et al., 1988).

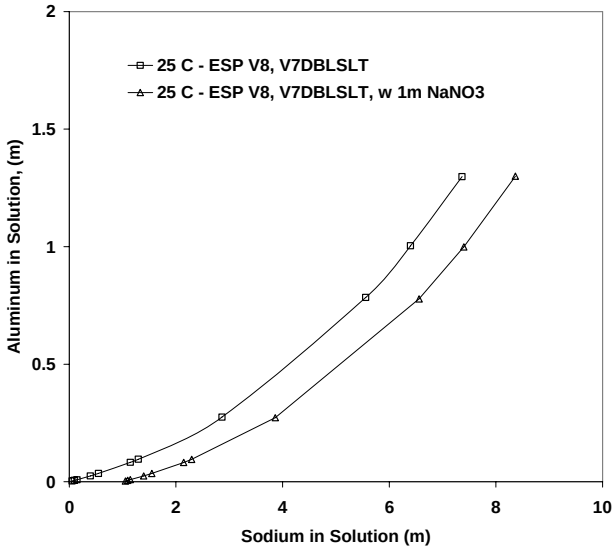

Figure 38. Comparison of ESP Predictions of Gibbsite Solubility in Presence of Sodium Nitrate (horizontal axis is sodium molality in solution).

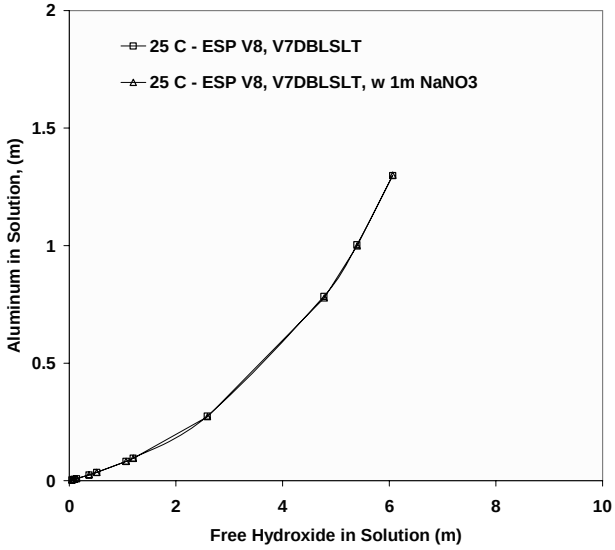

Figure 39. Comparison of ESP Predictions of Gibbsite Solubility in Presence of Sodium Nitrate (horizontal axis is free hydroxide molality in solution).

The presence of a variety of sodium salts (sodium nitrate, sodium nitrite, sodium carbonate and sodium sulfate) on the solubility of gibbsite in caustic solutions was examined through prediction using ESP. Although there was no significant difference between the predicted solubility of gibbsite in caustic solutions and in caustic solutions containing 1 m sodium nitrate (Figures 38, 39), the presence of multiple sodium salts at levels where the solution is saturated in these species does give rise to predictions for gibbsite solubility that are significantly different. Gibbsite solubility was predicted in solutions saturated with these sodium salts using ESP V8, and these predictions are compared to gibbsite solubilities in caustic solutions containing none of

these sodium salts. A comparison of the predictions is shown in Figure 40. Also shown in Figure 41 are predictions carried out with the proposed test plan maximum molalities of sodium nitrate (3m), sodium nitrite (1.5m) and sodium carbonate (0.5 m) At these loadings, the free hydroxide necessary to stabilize the aluminum in solution is reduced as compared to in the absence of these species. However, the free hydroxide requirement predicted for a solution fully saturated with these species is still larger than for the solutions containing the proposed loadings of sodium nitrate, sodium nitrite and sodium carbonate.

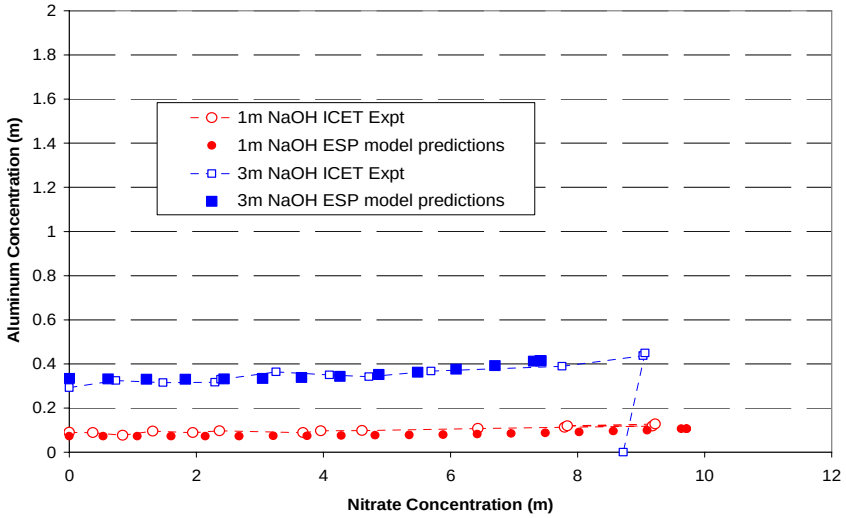

Figure 40. Prior Experimental Data for Gibbsite Solubility in 1 and 3 m Caustic at 25 °C in the Presence of Sodium Nitrate.

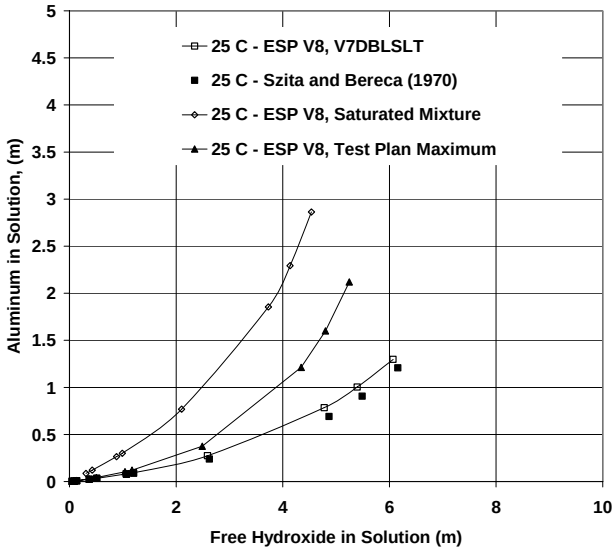

Figure 41. Comparison of Predictions for Gibbsite Solubility in a Saturated Solution Containing $NaNO_3$, $NaNO_2$, Na_2SO_4 and Na_2CO_3 and in Solutions Containing Proposed Test Plan Maximum Concentrations.

Establishment of Examined Concentrations for Test Plan

The WTP flow sheet information (Table 11) on the concentration ranges of important constituents with respect to aluminum solubility was received from Hanford [8]. Further discussions with site personnel identified sodium nitrate, sodium nitrite and sodium carbonate as the species to be examined as well as molality ranges for each species.

A statistical approach to the experimental design was recommended. Three temperatures (25, 40, and 55°C) and four caustic loadings (0.5, 1.5, 3.5, and 5.5 m) will be examined to allow coverage of the anticipated processing range(s) of WTP. Using the Taguchi method as implemented in the JMP 5 software program, a three level design for three variables (NO_3^-, NO_2^-, and CO_3^{2-} concentrations) was established. The three levels [High, Medium, and Low], resulted in a matrix of 9 experiments and are shown in Table 12. Additionally, a sample containing the High level for each constituent was added to the matrix, resulting in 10 experimental samples. This matrix will be replicated at each caustic loading and at each temperature. One series constitutes one caustic/aluminum loading at one temperature. Thus, there are four series performed at each temperature. All samples will be prepared in duplicate, resulting in 80 samples per temperature. Table 13 provides a compilation of the experimental concentrations for each anion to be employed in a given series.

Table 11. UFP1 and UFP2 Leaching Concentrations in mol/kg H_2O in Ion Exchange Feed.[2]

Analyte	UFP-1 Leaching		UFP-2 Leaching		Overall Range	
	mol/kg H_2O	mol/kg H_2O	mol/kg H_2O	mol/kg H_2O	mol/kg H_2O	mol/kg H_2O
	min	max	Min	max	Min	max
Na	8.10E-01	6.20E+00	1.92E+00	6.74E+00	8.10E-01	6.74E+00
K	8.77E-04	6.92E-01	1.23E-03	3.45E-01	8.77E-04	6.92E-01
Si	8.68E-04	6.70E-02	2.31E-03	3.78E-02	8.68E-04	6.70E-02
$Al(OH)_4$	3.60E-02	7.04E-01	1.26E-01	4.86E-01	3.60E-02	7.04E-01
OH	4.33E-01	5.46E+00	1.45E+00	4.40E+00	4.33E-01	5.46E+00
NO_2	4.78E-09	7.96E-01	1.18E-02	6.60E-01	4.78E-09	7.96E-01
NO_3	4.28E-03	1.81E+00	1.86E-01	1.64E+00	4.28E-03	1.81E+00
CO_3	2.95E-09	5.20E-01	6.32E-05	2.31E-01	2.95E-09	5.20E-01
PO_4	3.18E-03	1.63E-01	1.13E-02	1.29E-01	3.18E-03	1.63E-01
SO_4	1.82E-03	9.98E-02	1.17E-02	1.60E-01	1.82E-03	1.60E-01
Cl	7.31E-03	9.90E-02	2.43E-02	1.09E-01	7.31E-03	1.09E-01
F	3.54E-03	3.05E-01	1.17E-02	5.15E-01	3.54E-03	5.15E-01
C_2O_4	1.66E-03	1.07E-01	5.11E-03	2.52E-02	1.66E-03	1.07E-01
TOC	1.23E-03	6.87E-01	1.94E-03	3.74E-01	1.23E-03	6.87E-01
wt% H_2O	72.0%	95.6%	72.5%	90.3%	72.0%	95.6%

Ionic Strength	8.95E-01	7.49E+00	2.33E+00	7.05E+00	8.95E-01	7.49E+00
density (kg/L)	1.04	1.26	1.09	1.25	1.04	1.26

Table 12. Taguchi Experimental Design for 1 Series.

Point Number	NO_3^-	NO_2^-	CO_3^{2-}
1	M	L	L
2	L	M	L
3	L	H	M
4	M	H	H
5	L	L	H
6	H	L	M
7	M	M	M
8	H	M	H
9	H	H	L
10	H	H	H

Table 13. Molalities for Each Species.

Values (mol/kg H_2O)	NO_3-	NO_2-	CO_3^{2-}
High (H)	3.0	1.5	0.5
Medium (M)	1.5	0.75	0.25
Low (L)	0.0	0.0	0.0

Experimental Methods and Materials

Initial experiments with pure component aluminum and sodium hydroxide will provide the baselines for the aluminum solubility at the caustic loadings and temperatures selected. Experimental solubilities reported in the literature for aluminum or aluminate anion $[Al(OH)_4^-]$ at the caustic loadings of interest, started with either gibbsite, $Al(OH)_3$, or sodium aluminate, $NaAlO_2 \cdot 2.5H_2O$. In the planned experiments at ICET, aluminum wire will be used as the starting material. [9, 10] Using aluminum wire will result in the ability to independently establish the aluminum in solution without simultaneous addition of either sodium (if sodium aluminate is used) or hydroxide (if gibbsite is used).

Equilibrium for these experiments will be approached from above the solid-liquid equilibrium response curve and attainment of equilibrium will be established when the measured aluminum concentration is unchanged (within analytical error) after two or more weekly sample analyses. One sample at each condition will be prepared in a 250 mL vessel, which will be sampled weekly until equilibrium is ascertained. The initial volume of the sample will be prepared to ensure that removal of aliquots for analysis will not significantly change the overall composition in the sample. The second sample will be prepared in lesser amount in a 125 mL vessel, and will

be equilibrated without sampling until attainment of equilibrium has been established with the 250 mL sample.

Materials

Two liter solutions of 0.5, 1.5, 3.5, and 5.5m sodium hydroxide will be prepared using ACS reagent grade sodium hydroxide pellets and degassed DI (Millipore Milli-Q system) water. Molality will be the concentration method used in order to allow mass balance closure. The density of each solution will be measured prior to and after addition of all components. Pure aluminum wire (Fisher Scientific ACS certified) will be degreased with ethanol, dried, and weighed for each hydroxide solution. [9, 10] ACS reagent grade $NaNO_3$, $NaNO_2$, and Na_2CO_3 (anhydrous) will be heated to remove any possible water and stored in a dessicator until use. Individual experimental solutions will be prepared in either 125 or 250 mL PMP (polymethylpentene) vessels.

Preparation of Solutions

Aluminum wire will be added to the sodium hydroxide solutions such that the solutions will be supersaturated with Al. The initial aluminum input values (see appendix 1) will be determined using OLI-ESP, Inc. model predictions with respect to keeping the caustic loading at a constant value after the aluminum wire is added and dissolved, and solids are predicted. Results obtained from the pure component solutions will be used for the mixed solution experiments. In this case, care will be given such that the initial aluminum redox reaction is complete prior to adding additional components. Densities and percent water will be obtained from undiluted samples and the corresponding weights (molal) for each component will be added to 100 g (or 200 g for sampling vessel) of Al/OH solution. Each solution will then be placed in an incubator/shaker at constant temperature during the equilibration period.

Analytical Measurements

Aliquots will be taken weekly via syringe (loaded with DI water and weighed) or calibrated pipette from the duplicate set of samples. For each sample, density will be measured either by weight (diluted at higher temperatures) or undiluted if a density meter becomes available. Percent water will be obtained using thermogravimetric (TGA) measurement of solutions. Each sample will be analyzed for $OH^-/AlOH_4^-$, CO_3^{2-} (diluted) via accepted titration methods, inductively-coupled plasma optical emission spectroscopy (ICP-OES) will be used for Na, Al ions (diluted), total inorganic carbon/total organic carbon (TIC/TOC) measurements will be performed for C, and ion chromatography (IC) will be used for all other anions. Initial dilutions are typically 1mL solution to 9 mL DI water. Additional dilutions may be necessary for ICP, IC, and TIC analyses. Solids identification will be obtained using PLM imaging, ICP-OES and if possible, XRD. The aliquot amounts will be dependent upon the presence of solids and if filtration is needed.

Secondary Aluminum Experiments

Due to aluminum measurement concerns for systems approaching equilibrium from the top down, additional experiments will be prepared using gibbsite as the starting material and having the same sodium salt compositions as noted above, in order to approach the solid/liquid equilibrium from the bottom up. The solutions will be prepared using ACS reagent grade sodium hydroxide, sodium nitrate, sodium nitrite, sodium carbonate (anhydrous), and crystalline gibbsite (product number C-333) kindly provided by Almatis and published procedures. [11]

APPENDIX -1

Description of ESP experimental model set up for the pure component (Na-Al-OH-H_2O) system designed to maintain a constant free hydroxide loading begins by inputting the minimum values for water, sodium hydroxide, and aluminum wire. Initial input values for a 1.0 molal free hydroxide solution included 1000 g water, 40 g (1 mole) sodium hydroxide, and 2.04 g (0.076 mole) aluminum wire. Literature values for gibbsite in 1 m hydroxide at 25 °C were used as the aluminum starting point for these calculations. The hydroxide and aluminum wire weights were then tuned until the final output for free hydroxide was 1 molal and gibbsite solids were predicted. For the model output shown below, final input values used were 1000 g water, 42.5 g sodium hydroxide, and 6.5474 g aluminum wire.

Temp, C	25
Pressure, atm	1
pH	13.8426
Ionic Strength	0.018683
Aqueous	
	g/hr
H2O	986.2806
H2	0.001335
ALOH3	2.46E-07
OHION	16.80314
ALOH2ION	1.92E-15
ALOH4ION	7.08633
ALOHION	1.38E-24
H3OION	2.94E-13
NAION	24.42859
Total g/hr	1034.6
Volume, L/hr	0.989934
Density, g/L	1045.12
Solid	
ALOH3	13.6831
Total g/hr	13.6831
Volume, L/hr	0.005606
Density, g/L	2440.66

Vapor	
H2O	0.209952
H2	0.754645
Total g/hr	0.964597
Volume, L/hr	9.4499
Density, g/L	0.102075

Upon the preparation of approximately two liters of this aluminate/hydroxide solution (stock), 200 g will be charged to weighed vessels for immediate addition of the sodium salts. Stock solutions will enable consistent water loadings for all samples within a series. Since molality is the concentration used, the sodium salts additions will be based upon %water in the solution for all experimental samples. For example, since ESP predicts 95.3% water by weight for the free hydroxide solution (actual experimental samples will use the TGA results), 49.8 g $NaNO_3$ (3.0 molal), 20.2 g $NaNO_2$ (1.5 molal), and 10.1 g Na_2CO_3 (0.5 molal) would be added stepwise until all salts are in solution for the high/high/high value sample. All experimental samples will be prepared in a likewise manner.

WORK PLANNED FOR NEXT QUARTER

Upon receipt of equipment, 25°C samples will be prepared as described. Bi-weekly sampling will be done until solutions have reached equilibrium. All experimental data will be compiled and shared with site personnel as well as prepared for regressions with available literature data.

CONCLUSIONS

A test plan was compiled following suggestions and input from site personnel as well as input from reviewers. Upon corrections and additional information to this test plan, all participants were sent copies in accordance to the deliverable milestone requirement.

REFERENCES

1. Barney, G.S. "Vapor-Liquid-Solid Phase Equilibria of Radioactive Sodium Salt Wastes at Hanford," ARH-St-133, Dist. Cat. UC-4, Atlantic Richfield Hanford Company, Richland, WA, 1976.
2. Ruff, T. J.; Toghiani, R.K.; Smith, L.T.; and Lindner, J.S. "Studies on the Gibbsite to Bohemite Transition," *Sep. Sci. and Technol. 43*(9-10), **2008**, 2887-2899.
3. Selvaraj, D.; Toghiani, R. K.; and Lindner, J.S. "Solubility in the $Na+F+NO_3$ and $Na+PO_4+NO_3$ Systems in Water and in Sodium Hydroxide Solutions." *J. Chem. Eng. Data* 53(6), **2008**, 1250-1255.
4. Toghiani, R. K.; Phillips, V. S.; Smith, L. T.; and Lindner, J. S. "Solubility in the $Na+SO_4+NO_3$ and $Na+SO_4+NO_2$ Systems in Water and Sodium Hydroxide." *J. Chem. Eng. Data*, 53(3), **2008**, 798-804.
5. Toghiani, R. K.; Phillips, V. S.; and Lindner, J. S. "Solubility of $Na-F-SO_4$ in Water and in Sodium Hydroxide Solutions." *J. Chem. Eng. Data*, 50, **2005**, 1616-1619.

6. Smith, L.T.; Ruff, T.J.; Phillips, V.; Jung, M.; Toghiani, R.K., and Lindner, J.S. "Aluminum Solubility," *presentation*, Aluminum Chromium Leaching Workshop, Hosted by Savannah River Site, Atlanta, GA, January, 2007.
7. Apps, J.A., Neil, J.M., Jun, C.H., "Thermochemical Properties of Gibbsite, Bayerite, Boehmite, Diaspore, and the Aluminate Ion between 0 and 350 C", Technical Report, LBL-21482, August 1998.
8. Personal communication, *Draft Sodium Assessment Report*, J. Reddick, Hanford.
9. Sipos, P., Hefter, G., and May, P.M. "A Hydrogen Electrode Study of Concentrated Alkaline Aluminate Solutions", *Aust. J. Chem*, 1998, **51**, 445.
10. Li, H., Addai-Mensah, J., Thomas, J.C., and Gerson, A. R. "The influence of Al(III) supersaturation and NaOH concentration on the rate of crystallization of $Al(OH)_3$ precursor particles from sodium aluminate solutions", *J. of Coll. and Int. Sci*., 2005, 286, 511.
11. Reynolds, D. R. and Herting, D. L., "Solubilities of Sodium Nitrate, Sodium Nitrite, and Sodium Aluminate in Simulated Nuclear Waste," Technical Report, RHO-RE-ST--14P, September, 1984.

In-tank/At-tank Characterization for Closure of Hanford Tanks

David L. Monts, Ping-Rey Jang, and Zhiling Long

INTRODUCTION

The goal of this project is to develop and deploy in-tank waste characterization tools for use at the Hanford Site. These will be used to reduce uncertainties and risks associated with waste processing and closure activities. Some of the systems developed for this effort are also applicable to other DOE sites, such as Savannah River.

After as much waste as practical has been removed from the tank, analyses of remaining deposits will be needed to determine the long-term risk associated with the residual waste and to determine the appropriate steps required for closure. These needs are described in Hanford Technical Challenges WT-115, Technology to Support Post-Retrieval Evaluation of SSTs and in DOE-EM Engineering & Technology Roadmap, Improve Residual Waste Tank Characterization and Stabilization.

ICET will assemble and test a quantitative imaging system for demonstration as a nondestructive, *in situ* means of determining the volume and height of waste (including that deposited on tank walls), based on Fourier-transform profilometry (FTP). FTP images are obtained by using a white light source to project a fringe pattern onto the object of interest and using a camera to record the resulting distortions of the fringe pattern due to reflection from non-flat surfaces. A software package has been developed that automatically processes the FTP image to yield quantitative measurements and renderings of the object. FTP will provide quantitative spatial distribution determination of residual waste deposits. FTP will be tested under simulated Hanford conditions and its performance (accuracy, precision, etc.) will be documented. The FTP will thereafter be demonstrated at an appropriate location as a step toward ultimate deployment in actual Hanford waste tanks.

The FTP effort will complete a series of performance evaluation tests. The purpose of these tests is to document the accuracy, precision, and operational performance using blind testing techniques. Nondescript targets will be created and their volumes determined by traditional methods. The first testing stage involved objects on the bottom of a flat simulated C200-series Hanford waste tank and analyses from single FTP images. The second stage involves using new non-descript targets and determining the total volume present by “stitching” the results of individual images together for a flat tank bottom. The third stage involves volume determinations from a single image of nondescript targets on a simulated curved tank bottom, similar to those found in a variety of Hanford tanks. The fourth stage combines “stitching” of results of individual images acquired using a simulated curved tank bottom. These tests will demonstrate the performance of the FTP system prior to demonstration at an appropriate location. The FTP

effort is conducted with consultation with our Hanford collaborators. The ICET FTP probe system will be tested and optimized under simulated conditions at ICET (Stage 5 performance evaluation). The FTP effort will continue our research on improving phase-unwrapping algorithms, on image-quality improvements, and on development of algorithms to remove image noise.

WORK ACCOMPLISHED

During this quarter, substantial progress was made on the FTP technical feasibility study initiated during the previous quarter and requested by our Hanford collaborators. During the fourth quarter of 2008, the FTP prototype system was successfully used to perform volume determinations under conditions corresponding to the most challenging within a Hanford waste tank, i.e., ~53 feet away from a non-descript target at an angle of ~62° for a system that is 9 ft away from the tank center and also 25 ft above the tank floor. In the last quarterly report, it was noted that although the volume errors were small (on average about 8%), a systematic error was apparent: FTP volume determinations were made at three different projector-to-camera separations *d*; for the largest and small separation, all the volume errors were positive, while for the intermediate separation, all the volume errors were negative. During the current quarter, extensive efforts were made to understand the source of the systematic error.

These efforts evolved into a fresh characterization of the inherent and instrumental uncertainties associated with the current FTP system; this is necessary because previous characterization of instrumental response had been performed over the years with a variety of different equipment and different experimental configurations, rendering comparisons and generalized quantitative conclusion difficult. Consequently, a comprehensive campaign was begun. Using standard targets (solid cones), the FTP volume error was characterized as a function of stand-off distance. Analysis of five different images of three different targets at standoff distances of 7, 14, and 21 feet yielded average volume errors of about ± 2% with a standard deviation of 1-3%.

The sampling frequency was also investigated [2]. The signal includes not just the fundamental of the fringe pattern at spatial frequency f_0, but also harmonics at 2 f_0, 3 f_0, etc. In order to separate out the nth harmonic, it is necessary that the ratio m of the sampling frequency to the fundamental fringe frequency f_0 be

$$m \geq \frac{4}{3}(n+1) \qquad (1)$$

For n =3, m must be greater than about 5.33; for n = 2, m must be greater than about 4.0. In general, only the n = 2 harmonic has any significant intensity. As is shown in Table 14, the sampling frequency is more than sufficient to cleanly separate the fundamental spatial frequency f_0 from the harmonic frequencies; this is essential for accurate Fourier transform analysis of the images.

Table 14. Experimental ratio *m* of sampling frequency to fundamental spatial fringe frequency f_0 as a function of distance. L = camera-to-object distance.

Distance L (cm)	f_0 (lines/cm)	Pixels/cm	*m*(expt.) (pixels/line)
232.6	3.481	21.9	6.3
434.8	1.863	20.2	10.8
652.4	1.233	26.7	21.7
1615.6	0.747	33.5	44.8

A poster describing the FTP technical feasibility study preliminary results was presented at the 2009 Waste Management conference [1].

CONCLUSIONS

A fresh characterization of the inherent and instrumental uncertainties associated with the current FTP system is necessary because previous characterization of FTP instrumental response had been performed over the years with a variety of different equipment and different experimental configurations, rendering comparisons and generalized quantitative conclusions difficult. The characterization results will enable us to quantify the factors affecting the FTP volume measurement uncertainty and to develop a more robust FTP system with improved performance.

WORK PLANNED FOR NEXT QUARTER

During the next reporting period, the effect of imager stability will be investigated. The effects of camera zoom, camera shutter speed, fringe pattern focus, and fringe pattern uniformity on measurement uncertainty will be characterized.

REFERENCES

1. David L. Monts, Ping-Rey Jang, Zhiling Long, O. Perry Norton, Walter P. Okhuysen, Yi Su, and Charles A. Waggoner, "Technical Performance Capability of Fourier Transform Profilometry for Quantitative Waste Volume Determination under Hanford Waste Tank Conditions," *Proceedings of 35th Waste Management Symposium (WM'09)*, March 1-5, 2009, Phoenix, AZ, Paper No. 9333.
2. Chen, Wenjing, et al., "Error Caused by Sampling in Fourier Transform Profilometry," Optical, Engineering, 38(6) 1029–1034 (1999)

NOMENCLATURE

DOE	U.S. Department of Energy
EM	Environmental Management
FTP	Fourier transform profilometry

ICET	Institute for Clean Energy Technology
SST	single shell tank
WT	Waste Treatment

Laser Induced Breakdown Spectroscopy: Application to Nuclear Waste Management

J.P. Singh, F.Y. Yueh

INTRODUCTION

The use of a laser to produce a micro-plasma to vaporize, dissociate, excite or ionize species on material surfaces is known as laser induced breakdown spectroscopy (LIBS). The study of the atomic emission from the micro-plasma provides information about the composition of the material. LIBS is suitable for rapid on-line elemental analysis of any material phase and has value in obtaining analytical atomic emission spectra directly from solid, liquid, and gaseous samples.[1-3] The laser light and emitted signal can be delivered via optical fiber so LIBS can be used in hazardous environments. It is a fast qualitative analysis technique that has been used on a variety of samples such as polluted soils, Mars surface, alloy, glass, explosive, tissues, etc. In some solid samples, LIBS has demonstrated an accuracy of 3-6% for elements with a concentration greater than 1 wt% and an accuracy of 5-10% or better for minor elements depending on their concentration (based on 2.5 error confidence).[4,5] The technique satisfies the needs for industrial processes and environmental monitoring due to its remote, real-time, multi-elements capability. Despite having lower figures of merit than other elemental techniques, the method satisfies the needs for industrial processes and environmental monitoring due to its remote, real-time, multi-elements capability. Additionally, the technique is less complicated than a number of laser-based instruments, and is cost-effective.

WORK PERFORMED

The direct analysis of slurry samples using LIBS present some challenges such as sedimentation, splashing, surface turbulence, and decreased S/N due to weaker laser induced plasma. Previously circulation systems and direct sampling technique for LIBS measurement have been evaluated and found that due to high water content the laser shock wave caused splashing resulting in large measurement variation. In addition, particle settling or sedimentation makes bulk analysis with LIBS difficult. In this work period, an investigation of how water content affects the LIBS signal was performed and various techniques to reduce water content in slurry samples were evaluated. The slurry sample used was prepared by Smith et al. [6] and was based on the recipe for simulated Tank 8F (SRS) sludge containing no RCRA metals or Halides.

[7] The slurry has been analyzed by ICET analytical laboratory. It contains ~79% water and the results of slurry analysis (dry based) are given in Table 15. To study the effect of water on the LIBS signal, a ~1 ml slurry sample was placed in a 3-cm beaker in a furnace at the set temperature 80°C to evaporate water. A small amount of the sample after the heat treatment was analyzed by a thermogravimetric analyzer (TGA) to determine the water content left after heating. The rest of the heated sample was used for LIBS measurement. The beaker was on a rotating stage during measurement to make sure each measurement is from a new location. Figure 42 shows the LIBS signal obtained from four samples with different drying times. It is clear that the signal from samples with water content of 71 wt. % and above is very weak. The signal increased as the water content was reduced. These data show that LIBS signal has increased about 10 times by reducing water to a level of about 50%. Improved reproducibility was also observed as water content was reduced.

Table 15. Concentration of Sludge Feed Simulants (wt%, dry)

Al	7.37
Ca	2.09
Cu	0.14
Fe	24.2
K	0.042
Mg	0.145
Mn	2.4
Ni	2.67
Si	0.813
Sr	0.085
Zn	0.266

* Slurry Water Content: 79%

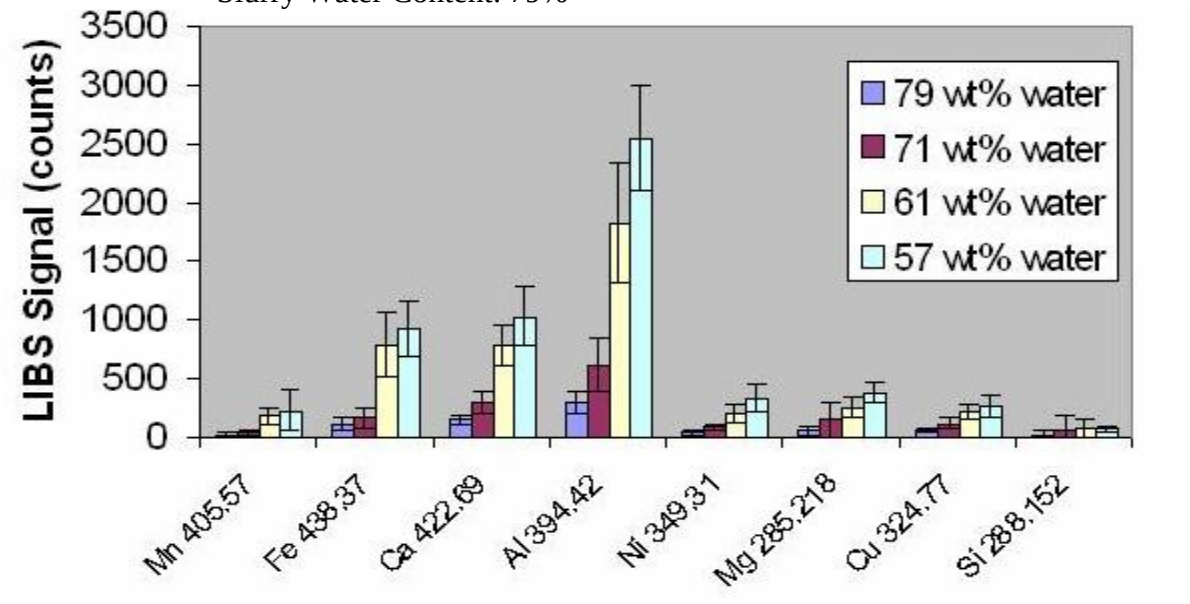

Figure 42. Effect of Slurry Water Content on LIBS Signal. The numbers following the element symbol are the emission line analyzed.

The initial test results show that reducing the water loading can improve the laser measurements. Three sample preparation methods to reduce sample water content provide good signal-to-noise and reproducibility data are now under evaluation. The details of these methods are outlined in Table 16. In the first method, a slurry of ~ 50 wt.% water was prepared by heating the slurry in a beaker at 80°C. This process took about 20 minutes for a 1- gram sample (79 to about 50 wt.% water. After some water evaporated from the sample, it also resulted in many cracks on the sample surface (see photo, top panel of Figure 43). The second method used a double-sided tape on a glass slide to hold ~ 20mg slurry. Repeated tests show that placing the glass slide on 50 °C hot plate for two minutes produced consistent LIBS results. In the third method, the tape was replaced with a thin layer of PVC. The slurry on PVC was heated at 50 °C for 5 minutes before the actual measurement. More than ten samples with each sample preparation method were prepared. The data of these samples was collected and the signal and relative standard deviation (RSD) are compared (see Figure 43). It is clear that LIBS signal from method 1 (i.e. slurry in beaker) gave the poorest signal and reproducibility. The relatively higher water content and many cracks that formed on the sample surface produced an uneven target. The slurry sample used in these tests contains low Si (see Table 16). Therefore, the Si signal should be low from these samples. However, a strong Si signal from some single shot data was observed. This indicates that the data with strong Si signal is not produced from sample but from the beaker. The signals obtained from slurry on PVC are slightly stronger than the signal from slurry on the double-sided tape; however, the slurry on the double-sided tape required the shortest sample prepetition time. The data from this later technique yielded ~3 times higher analyte signal and ~ 2 time lower standard deviation as compared with the results from sample prepared with method 1.

Table 16. Three sample preparation methods tested.

Slurry Sample	Sample inside a beaker	Sample on double sided tape	Sample on PVC
Sample Weight (g)	~1g	< 0.02g	~0.02g
Sample preparation procedure	1. place ~1ml slurry in 3-cm beaker 2. place the beaker in side a 80C furnace for 20 minutes20 min	1. Put double sided tape on a glass slide 1. Spread a drop of slurry on a glass slide with double sided tape 2. put glass slide on a 50C hot plate for 2 minutes	1.Put a thin layer of PVC on a glass slide; wait 5 minutes 2. Spread a drop of slurry on a glass slide with PVC sided tape 3. put glass slide on a 50C hot plate for 5 minutes
Water content after Sample preparation	~50-60 w% (based on TGA)	<10 w% (based on weight loss after drying)	<10 w% (based on weight loss after drying)

Slurry sample after preparation	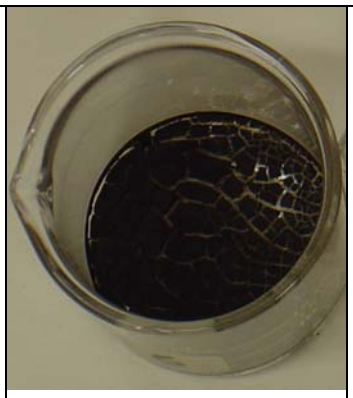		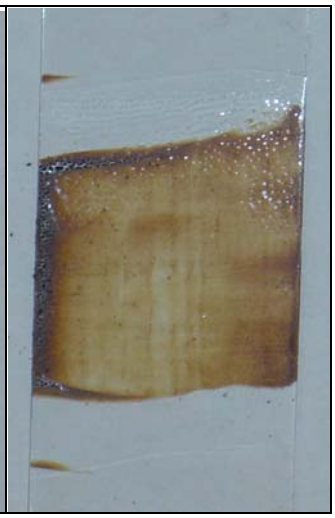

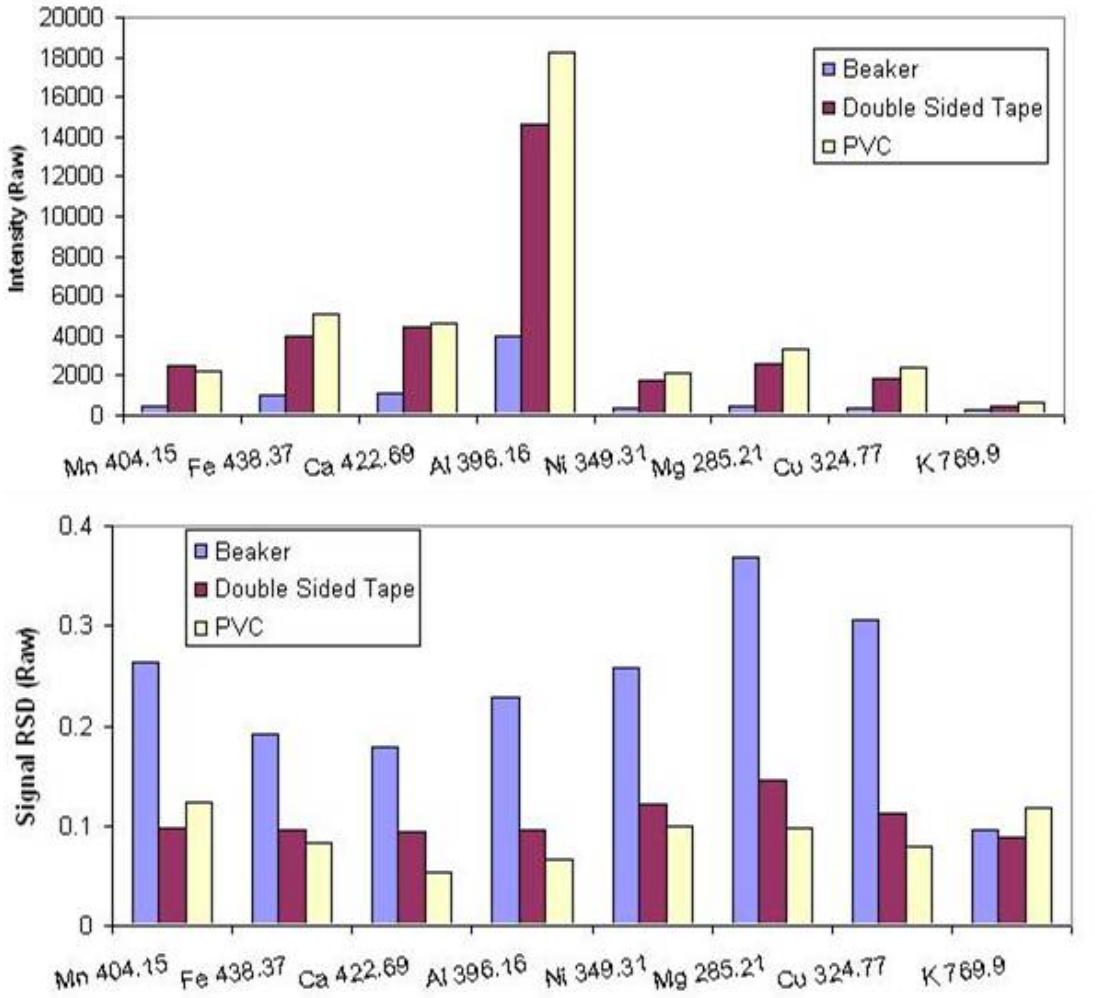

Figure 43. The averaged LIBS signal and relative standard deviation from ten samples of each sample preparation method.

It is known that laser plasmas have poor reproducibility due to laser shot-to-shot variation. To obtain quantitative results with LIBS, normalization techniques are generally used to account for matrix effects, plasma fluctuation, and ablation rate. There are different types of normalization techniques that have been employed [8-13]. The integrated plasma emission normalization usually works well for the samples that have similar physical and chemical properties. This corrects for the variation on ablation rate and small variation on plasma characteristic due to laser energy fluctuation. Other common normalization techniques used in LIBS include the use of an internal standard, normalization to the acoustic signal from plasma ignition, and using simultaneously recorded plasma characteristics. Hung and Lin has shown that analysis of plasma-induced current signals, taking into account the ablated amount of microdroplets and the plasma excitation temperature, retains correlation linearity over a much wider range of laser energy [13]. In an earlier slurry study, it was found that with plasma emission normalization (integrated emission from the selected wavelength ranges) improvements in both the linearity of the calibration curve and the reproducibility of the results was possible [14]. From Figure 43 it is seen that 10-40% RSD from these three sample types is possible. To improve the measurement RSD, plasma emission normalization was applied to all the data and the results are shown in Figure 44. In this case, the sample-to-sample variation was reduced and differences between the different sample preparation methods were minimized. The RSD has improved to below 10% for method 1 and 5% for methods 2 and 3 for most analyte lines. Please note, although the averaged normalized signal from the data of three sample preparation methods are comparable, the data from samples prepared with method 1 has poorer sensitivity due to low signal-to-noise. The preliminary test in this work period shows that the sample preparation methods 2 and 3 both give reasonably good signal-to-noise ratio and reproducibility. Continued evaluation of methods 2 and 3 involving substrate deposition are planned.

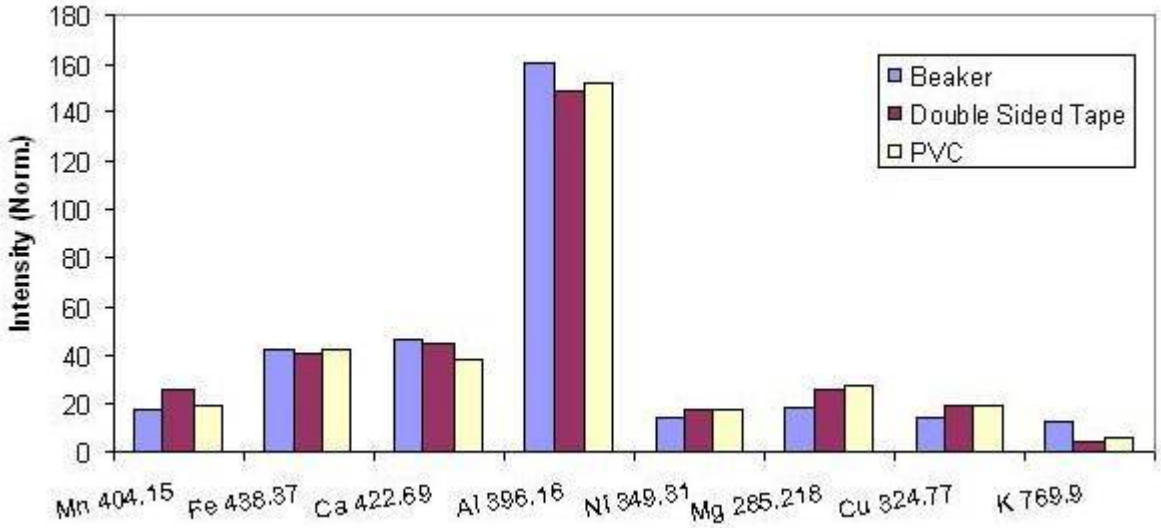

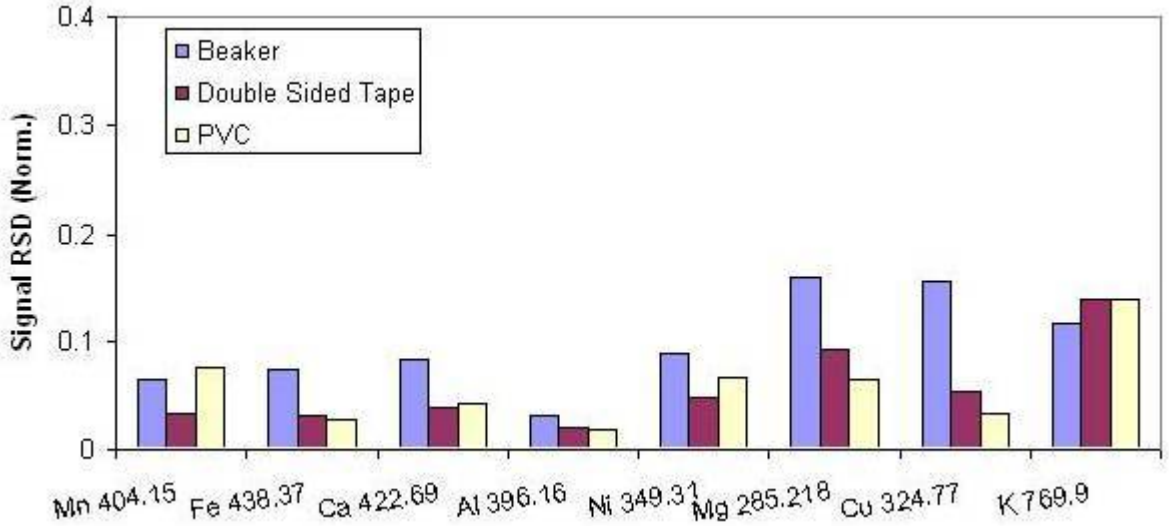

Figure 44. The normalized LIBS signal and relative standard deviation from ten samples of each sample preparation method.

CONCLUSION

The original slurry samples contain high water content; water can affect the density, and the thermal diffusivity of the sample, thereby affecting the energy density required for breakdown. The LIBS signal was observed to increase as the water content was reduced. Efforts to improve measurement quality by reducing slurry water content were made. It was found that the use of double-sided tape and PVC on a glass slide to probe the slurry sample shows the most promising results. Increased signal strength with minimal heating time was observed.

WORK FORECAST

Work to improve the performance of slurry measurement with different sampling methods and data processing techniques will continue.

REFERENCES

1. “Laser Induced Breakdown Spectroscopy” Editors Jagdish P Singh and S. N. Tahkur, (Elsevier, Amsterdam, 2007).
2. Fang-Yu Yueh, Jagdish P. Singh and Hansheng Zhang, "Laser-induced breakdown spectroscopy-elemental analysis", in *Encyclopedia of Analytical Chemistry*, R. A. Meyers, ed. (Wiley, New York, 2000).
3. A. Miziolek, I. Schechter and Peleschi, "Laser induced plasma spectroscopy: a review of recent advances, " Rev. Anal. Chem. 16, 173-298 (1997).

4. B. Lal, F. Y. Yueh, J. P. Singh, "Glass-batch composition monitoring by laser-induced breakdown spectroscopy", Appl Opt. 44, 3668-74 (2005).
5. H. Zheng, F. Y. Yueh, T. Miller, J. P. Singh, K. Zeigler and J. Mara, "Analysis of Surrogate of Plutonium (Pu) Residue Using Laser Induced Breakdown Spectroscopy", Spectrochimica Acta **63**, 968-974 (2008).
6. L. Smith, T. Ruff, V. Phillips, M. Jung, R. Toghiani, and J. Lindner, "Aluminum Solubility" , presentation at the Aluminum Chromium Leaching Workshop, Atlanta, GA 2007.
7. M. R. Poirier, Recipe for Simulated Tank 8F Sludge Containing No RCRA Metals or Halides,WSRC-TR-2005-00045 Rev.0, Westinghouse Savannah River Company, Aiken SC.
8. Gornushkin et al., "Effective normalization techique for correction of matrix effects in laser-induced breakdon spectroscopy detection of magnesium in powdered samples", App. Spectrosc. 56(4), 433-436 (2002).
9. R. Barbini, F. Colao, R. Fantoni, A. Pallucci, F. Capitelli, Application of laser-induced breakdown spectroscopy to the analysis of metals in soils, Appl. Phys. A 69Ž1999. 175_178.
10. D. Body, B.L. Chadwick, Optimization of the spectral data processing in a LIBS simultaneous elemental analysis system, Spectrochimica Acta Part B 56, .725_736(2001)
11. D. W. Hahn, M. M. Lunden, Detection and Analysis of Aerosol Particles by Laser-Induced Breakdown Spectroscopy. Aerosol Science & Technology, Volume 33, Numbers 1-2 / July 1, 2000.
12. A. W. Miziolek, V. Palleschi, I. Schechter, "Laser-Induced Breakdown Spectroscopy: Fundamentals and Applications", (Cambridge Univ. Press, New York, 2006).
13. J.-S. Huang and K.-C. Lin, Laser-induced breakdown spectroscopy of liquid droplets: correlation analysis with plasma-induced current *versus* continuum background, *J. Anal. At. Spectrom.*, 20, 53 – 59 (2005).14. S. Y. Oh, F. Y. Yueh, J. P. Singh, C. C. Herman and K. Zeigler, Preliminary evaluation of laser induced breakdown spectroscopy for slurry samples, Spectrochimica Acta Part B: Atomic Spectroscopy, 64(1), 113-118 (2009).

Evaluation of HEPA Filters Under Fire (High Soot Loading) Conditions

R. Arunkumar and C. A. Waggoner

INTRODUCTION

HEPA filters are used as the final element in nearly all containment systems where radioactive wastes are processed. The ability of these units to reduce the amount of particulate matter emitted from such processes is recognized as the most cost effective manner to achieve ALARA protection of workers and the environment.

Design of HEPA filtered ventilation systems receives great scrutiny with respect to the impact of fire and smoke from within containment of processes involving radioactive materials. Nuclear grade HEPA filters using fibrous glass media (ASME Standard AG-1, Section FC) are only rated to a maximum temperature of 350 degrees F, so controlling airflow temperature through the filter is important. Additionally, two other threats to system performance and integrity are associated with fires: (1) water damage of the filters and (2) rapid blinding of filters by soot.

Data are needed to aid in the development of loading models to incorporate the effects of water damage and filter binding on full size (24x24x11.5") as well as radial filters. Effective models are necessary for conducting reasonable and accurate reviews of vital safety systems involving HEPA filters. In this work, radial filters will initially be tested followed by testing of full size filters.

WORK ACCOMPLISHED

A new HEPA filter test facility has been designed to accommodate a nominal flow rate of 4000 scfm and allow for a differential pressure drop across a filter of 30 in. wc. A schematic of the facility is shown in Figure 45. Air is drawn from outside the building into a 24 in. diameter cross-sectional stainless steel pipe, following which smoke/carbon black or other aerosol simulant can be injected into the gas stream as a challenge. After a length of approximately 30 ft inside the building, the gas stream should be uniformly distributed. In case a longer mixing length becomes necessary, additional sections of pipe can be added outside the building upstream of the filter. To enable ease of handling, most of the test sections are 10 ft. in length and equipped with a suitable number of ports to permit extractive measurements from the gas stream. There is also provision for making temperature, pressure and humidity measurements. Once the stream passes through the filter, it is returned to the outside of the building using similar 24 in. cross-section pipes. All the air flowing through the system will be drawn through the system using a blower and the flow monitored using a venturi flow meter downstream of the test HEPA filter. Air flow rate control (using air bypass) on the test stand will be similar to what has worked

well on the existing (smaller scale) facility. This new facility has been designed to allow testing of both radial and standard filters.

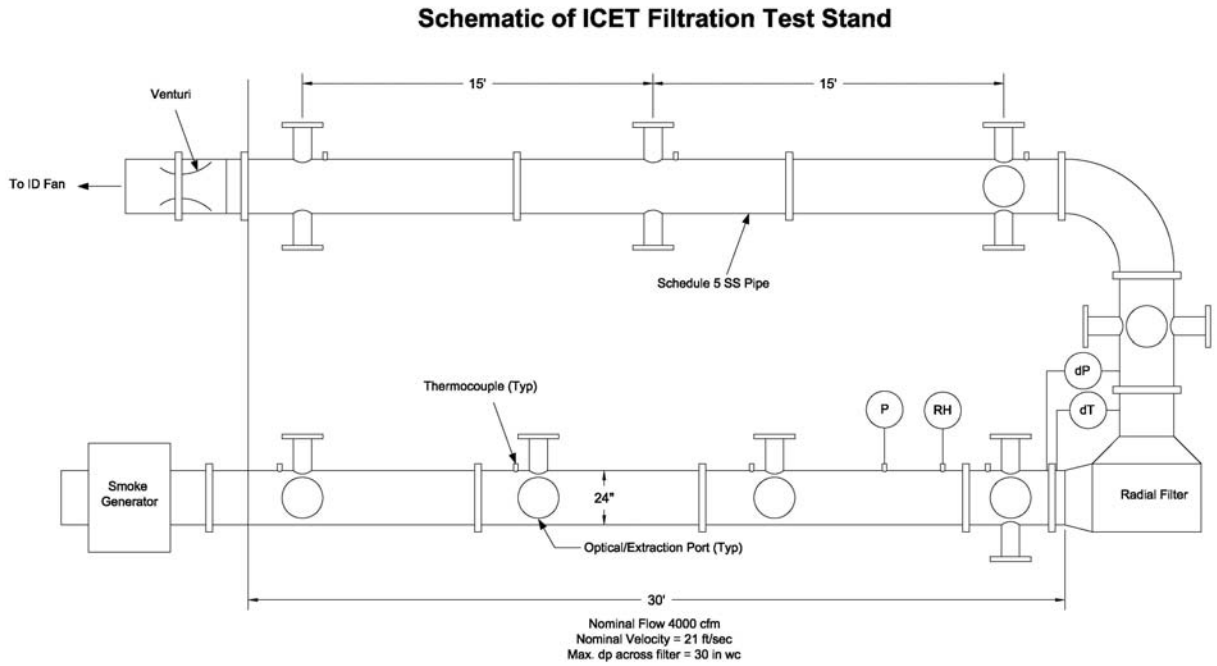

Figure 45. Schematic of ICET Large-scale HEPA Filter Test Stand

Measurement and control of the flow parameters will be performed on a Lonworks, network based system. Data will be acquired, logged and periodically backed up onto a data server with a personal computer. Data will be archived and available for retrieval at anytime for analysis.

Most of the elements of the facility are currently on order.

CONCLUSIONS

A new test facility has been designed and is being constructed in the high-bay area at ICET for challenging HEPA filters under fire (high soot loading) conditions. This facility will be under computer control and will allow for challenging of HEPA filters under heavy soot conditions (to simulate a fire).

WORK PLANNED FOR NEXT QUARTER

The next quarter will primarily be devoted to completing the construction and assembly of the test stand. When assembled we anticipate running our initial checkout tests of flow/flow control and soot distribution.

REFERENCES

1. Arunkumar, R., J. A. Etheridge, J. C. Luthe, B. A. Nagel, O. P. Norton, M.S. Parsons, D.M. Rogers, K. U. Hogancamp, and C.A. Waggoner, "Evaluation of Emissions from HEPA Filters as a Function of Challenge Conditions, Proceedings of the International Thermal Treatment Technologies Conference 2004, May 10-14, 2004, Phoenix, AZ.

Nomenclature

ALARA: As Low as Reasonably Achievable